Non-Coherent Successive Relaying and Cooperation: Principles, Designs, and Applications

Li Li, H. Vincent Poor, *Fellow, IEEE*, and Lajos Hanzo, *Fellow, IEEE*

Abstract—Cooperative communication is capable of forming a virtual antenna array for each node (user) in a network by allowing the nodes (users) to relay the messages of others to the destination. Such a relay aided network may be viewed as a distributed multiple-input multiple-output (MIMO) system relying on the spatially distributed single antennas of the cooperating mobiles, which avoids the correlation of the antenna elements routinely encountered in conventional MIMO systems and hence attains the maximum achievable diversity gain. Therefore, the family of cooperative communication techniques may be regarded as a potential solution for future wireless networks. However, constrained by the half-duplex transmit/receive mode of most practical transceivers, the cooperative networks may impose a severe 50% throughput loss. As a remedy, successive relaying can be employed, which is capable of mimicking a full-duplex relay and thereby recovering much of the 50% throughput loss. Furthermore, for the sake of bypassing power-hungry and potentially excessive-complexity channel estimation, noncoherent detection techniques may be employed for multiple-antenna aided systems, because estimating all the associated channels may become unrealistic. Explicitly, the mobile-stations acting as relays cannot be realistically expected to estimate the source-to-relay channels. To motivate further research on noncoherent successive relaying aided systems, a comprehensive review of its basic concepts, fundamental principles, practical transceiver designs and open challenges is provided.

AQ1   *Index Terms*—Author, please supply index terms/keywords for your paper. To download the IEEE Taxonomy go to http://www.ieee.org/documents/taxonomy_v101.pdf.

I. INTRODUCTION

CONCEIVING high-quality wireless solutions in support of the wireless Internet is of paramount importance. Achieving a low bit-error-rate (BER), high system throughput, low complexity, low delay, as well as seamless connectivity across the entire coverage area are just a few of the critical design concerns in contemporary wireless systems. It is anticipated that wireless tele-traffic will grow substantially over the forthcoming ten years [1, Figure 1]. Based on this trend, techniques that are capable of improving system capacity are of salient significance. In this context, multiple-input multiple-output (MIMO) wireless systems have attracted considerable attention in recent years [2]–[7], because they exhibit a capacity that increases linearly with the transmit power, provided that the number of MIMO elements can also be linearly increased.

However, the MIMO antenna elements have to be sufficiently far apart to experience independent fading, which may be impractical in the uplink owing to the limited size of the mobile handset. Furthermore, even a downlink MIMO base station (BS) transmitter associated with a relatively large element separation may not benefit from independent fading, when it is subjected to shadow-fading imposed for example by large-bodied vehicles or other local shadowing objects [8].

As a remedy, cooperative communications is capable of forming a virtual antenna array (VAA) for each node (user) in a cooperative network by allowing the nodes (users) to relay the messages of other's to the destination. Hence, such a relay aided network practically constitutes a distributed MIMO system relying on the spatially distributed single antennas of the mobiles. This allow us to avoid the correlation of the antenna elements that arises in conventional MIMO systems.

The germination of the basic idea of cooperative communication can be traced back to the concept of the relay channel, which was devised by Van der Meulen in [9] and was later characterized from an information-theoretic perspective by Cover and El Gamal in [10]. Basic relaying protocols were also proposed in [10]. To elaborate a little further, cooperative communications benefits from the broadcast nature of wireless transmitters, which allows the relays to receive and retransmit all signals, leading to the concept of "cooperative diversity". Laneman *et al.* characterised both the decode-and-forward (DF) and amplify-and-forward (AF) protocols in [11] and [12] by evaluating both their diversity orders and their outage probabilities. Similar concepts were investigated also by Sendonaris *et al.* in [13] and [14]. These seminal paradigms [11]–[14] have attracted substantial research attention and inspired a number of novel contributions in the research area of cooperative communications. Some of the important milestones achieved in the early stages of cooperative communications research are summarized in Table I.

However, despite the above-mentioned benefits, cooperation techniques impose their own problems as well. Since conventional transceivers cannot transmit and receive at the same time, we have to allocate two orthogonal channels for the reception

TABLE I
BRIEF HISTORY OF EARLY INVESTIGATIONS OF COOPERATIVE COMMUNICATIONS

Year	Authors	Contributions
1971	Van der Meulen [9]	Heralded the concept of cooperative communication and established the basic three-terminal relaying model.
1979	Cover and El Gamal [10]	Analysed the capacity of the three-terminal based relaying system along with proposing some basic relaying protocols.
2003	Sendonaris *et al.* [13], [14]	Evaluated the performance of several classical cooperative protocols. The remarkable advantages of cooperative communication were quantified in terms of their large power savings, low outage probability and high diversity order.
2004	Laneman *et al.* [12]	
2005	Azarian *et al.* [15]	Investigated the achievable diversity-multiplexing trade-off (DMT) of the cooperative network.
	Høst-Madsen and Zhang [16]	Optimum resource allocation was conceived for cooperative systems, which is capable of improving both the energy efficiency and battery recharge-period of cooperative communications.
2006	Bletsas *et al.* [17]	Relay selection regimes were exploited for improving the outage performance.

and transmission at the relay node (RN). Consequently, in the conventional cooperative protocols, such as in AF, DF as well as compress-and-forward [18] protocols, the holistic transmission of an information stream has to be split into two phases, namely the "broadcast phase" for the RN's reception and the "cooperative phase" for the RN's transmission. By contrast, the direct-transmission of the information stream dispensing with relaying requires only a single phase. Therefore, the conventional cooperation techniques actually impose a severe 50% throughput loss, which goes against the demand for higher wireless data rates, as highlighted in [1] and [19].

For the sake of recovering the throughput loss incurred in conventional half-duplex (HD) relaying based cooperation systems, while retaining their substantial benefits of extending the radio coverage, a range of advanced techniques have been proposed in recent years, which may be briefly categorised as follows:

(a) Switching to full-duplex (FD) relaying mode—In the early investigations of relaying techniques [9], [10], the idealized FD relaying mode was assumed for analysing the capacity upper-bound of relaying channels. However, from a practical perspective, relying on FD relaying may be infeasible for compact single-antenna aided relays. Since a high-power interfering signal will be fed back to the RN's input from the RN's output, this results in the so-called "self-interference" (SI) problem. Hence, instead of the FD mode, the HD mode has been employed in the seminal contributions on user cooperation [11]–[14], [20].

Nonetheless, with recent developments in digital signal processing techniques, mitigating the unwanted SI in the feedback path between the transmit antenna and receive antenna becomes possible. The related early results [21]–[23] were focused on realizing single-input single-output (SISO) repeaters. Later, the FD transceiver design philosophy was extended to multi-antenna aided spatial suppression techniques, which invoked more sophisticated adaptive filter algorithms [24]–[26]. Most recently, Katti *et al.* at Stanford made substantial progress in terms of building in-band full-duplex radios. Explicitly, with the aid of antenna cancellation techniques, they implemented in-band full-duplex transceivers [27]–[29], which are capable of reducing the SI to the noise floor. Motivated by the development of FD transceiver techniques, the theoretical analysis of FD
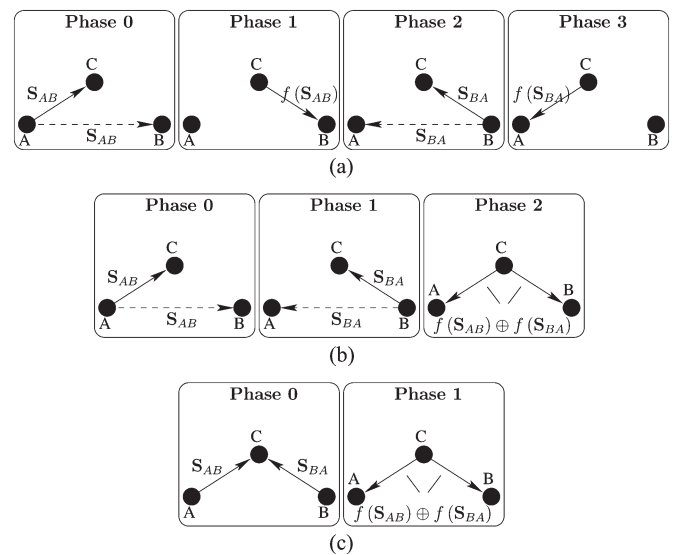

Fig. 1. The transmission arrangements of conventional DF relaying, three-step two-way relaying, and two-step two-way relaying while exchanging the information sequences fS_{AB} and $\mathbf{S}_{BA}$ between node A and B with the aid of the relay node C, where $f(\mathbf{S}_{AB})$ denotes the estimate of $\mathbf{S}_{AB}$.

relaying based cooperative networks enjoyed a renaissance in [30]–[32], where the impact of SI imposed by practical FD relays was taken into account.

However, as stated above, most of the proposed FD relays have to employ spatially separated transmit and receive antennas, which should have a sufficiently high physical isolation, whilst additionally relying on sophisticated adaptive filter algorithms. Hence, the implementation of FD relays still remains an open challenge at the time of writing and this motivates the design of alternative solutions.

(b) Devising sophisticated relaying protocols—For the particular scenario in which two nodes communicate with each other with the aid of a RN, "two-way" relaying was devised in [33]–[35], which has attracted considerable attention in recent years [36]–[40], since it inherently accommodates bandwidth-efficient network coding techniques. When exchanging the pair of information sequences $\mathbf{S}_{AB}$ and $\mathbf{S}_{BA}$ between node A and node B with the aid of the RN C, the transmission arrangements of conventional DF relaying and of two-way
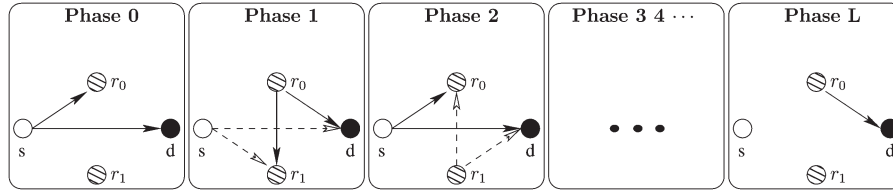
Fig. 2. Transmission schedule of the successive relaying protocol.

relaying are contrasted in Fig. 1. Observe in Fig. 1 that the four distinct transmission phases required by conventional DF relaying are compressed into three phases in the "three-step two-way relaying" regime or are further compressed into two phases in "two-step two-way relaying" regime. Hence the 50% throughput loss incurred by conventional relaying protocols is mitigated. In more detail,

1) **Three-step two-way relaying**: During Phase 0, the SN A broadcasts its information sequence $\mathbf{S}_{AB}$, while the RN C generates an estimate of $\mathbf{S}_{AB}$, namely $f(\mathbf{S}_{AB})$ relying on the signal sequence received.[1] Meanwhile, the DN B also obtains a copy of the information sequence $\mathbf{S}_{AB}$, which however may be contaminated both by the channel's fading effects and by additive white Gaussian noise (AWGN). Then, a similar process will be invoked again during the forthcoming Phase 1. This time, the SN becomes the receiver, the DN becomes the transmitter and the broadcast information sequence becomes $\mathbf{S}_{BA}$. As seen in sub-figure "(a) Conventional DF relaying" of Fig. 1, the RN C directly forwards the estimate $f(\mathbf{S}_{AB})$ or $f(\mathbf{S}_{BA})$ during its cooperative phase, which only bears the information of $\mathbf{S}_{AB}$ or $\mathbf{S}_{BA}$. By contrast, the RN C forwards the XOR of $f(\mathbf{S}_{AB})$ and $f(\mathbf{S}_{BA})$ i.e. $f(\mathbf{S}_{AB}) \bigoplus f(\mathbf{S}_{BA})$ during Phase 2 of the 3-step two-way relaying, which bears both the information of $\mathbf{S}_{AB}$ and that of $\mathbf{S}_{BA}$. Naturally, each node A and node B knows its own message $\mathbf{S}_{AB}$ or $\mathbf{S}_{BA}$. Hence each can readily extract the remote message by subtracting its own message from $f(\mathbf{S}_{AB}) \bigoplus f(\mathbf{S}_{BA})$. For example, assuming that perfect detection is achieved at the RN C, as well as that we have $\mathbf{S}_{AB} = \underbrace{0101}_{\mathbf{S}_{AB}}, \mathbf{S}_{BA} = \underbrace{1100}_{\mathbf{S}_{BA}}$, we readily see that $f(\mathbf{S}_{AB}) \bigoplus f(\mathbf{S}_{BA}) = \underbrace{1001}_{\text{XOR}}$. Hence, during Phase 2, node A becomes capable of recovering the remote message of $\mathbf{S}_{BA}$ by calculating $\underbrace{1100}_{\mathbf{S}_{BA}} = \underbrace{0101}_{\mathbf{S}_{AB}} \bigoplus \underbrace{1001}_{\text{XOR}}$. Practically, the XOR of $f(\mathbf{S}_{AB})$ and $f(\mathbf{S}_{BA})$ received at node A may also be contaminated both by the channel's fading effects and by the AGWN. Fortunately, as stated earlier, node A has another copy of its remote message, which was received during Phase 0. Hence a joint detection of the remote message based on both the signal received during Phase 0 and on that received during Phase 2 may be implemented at node A. Consequently, a diversity gain is obtained.

2) **Two-step two-way relaying**: During Phase 0, node A and node B simultaneously broadcast their information sequences $\mathbf{S}_{AB}$ and $\mathbf{S}_{BA}$. Limited by the HD transceiver architecture, neither node A nor node B can receive any signal during this phase. Meanwhile, the RN C receives a composite signal, which consists of the $\mathbf{S}_{AB}$ component and of the $\mathbf{S}_{BA}$ component. For the sake of calculating the XOR of $\mathbf{S}_{AB}$ and $\mathbf{S}_{BA}$, the RN C has to be able to detect each of the information sequences $\mathbf{S}_{AB}$ and $\mathbf{S}_{BA}$ from their composite.[2] Since the information sequences $\mathbf{S}_{AB}$ and $\mathbf{S}_{BA}$ interfere with each other at the RN C, interference cancellation has to be invoked at the RN C. Similar to the last phase of three-step two-way relaying, during Phase 1 of two-step two-way relaying, the RN C forwards the XOR of $f(\mathbf{S}_{AB})$ and $f(\mathbf{S}_{BA})$ to the DN A and B. Then, the DN A (B) extracts its own information sequence $\mathbf{S}_{AB}$ ($\mathbf{S}_{BA}$) from $f(\mathbf{S}_{AB}) \bigoplus f(\mathbf{S}_{BA})$ for the sake of decoding the information sequence transmitted by the remote node B (A). However, node A (B) receives only a single copy of the remote message during the two-step scheme, because the direct link between A and B becomes unavailable in Phase 0 of the two-step scheme owing to the HD limitation. Hence, compared to the three-step scheme, the two-step scheme completely recovers the throughput loss at the cost of degrading the achievable diversity gain.

However, the application scenario of the two-way relaying scheme is constrained to bidirectional communications.

(c) Mimicking the FD relaying mode despite relying on using HD relays—A novel relaying protocol, namely successive relaying or two-path relaying was conceived in [43], which is capable of mimicking a FD relay by relying on a pair of HD relays, where the two HD relays alternately serve as the transmitter and receiver of the virtual FD relay. Based on [43], as well as inspired by the related benefits reported in [33], [34], [44], and [45], a generalized successive relaying protocol was proposed by Fan *et al.* in [46], offering further insights both into the achievable rates and into the associated diversity versus multiplexing trade-off.

The transmission arrangement of the successive relaying protocol proposed in [46] is illustrated in Fig. 2, where we observe $(L + 1)$ processing phases. To elaborate a little further, observe in Fig. 2 that the SN s constantly transmits information during

---

[1]Hence, the decode-and-forward protocol is adopted at the RN C.

[2]In some studies, the DF protocol employed at the RN C is replaced by the AF protocol [41] or by the denoise-and-forward protocol [42]. Hence interference suppression for detecting each of the information sequences $\mathbf{S}_{AB}$ and $\mathbf{S}_{BA}$ at the RN is circumvented. Instead, the RN C may only amplify the composite signal received and forward it to node A and node B.

TABLE II
HISTORY OF SUCCESSIVE RELAYING

Year	Authors	Contributions
2004	Oechtering and Sezgin [43]	The concept of successive relaying was introduced, where a new cooperative transmission scheme was conceived.
2005	Rankov and Wittneben [33]	The benefits of employing successive relaying with regard to conventional relaying, especially the higher achievable throughput and the better diversity-multiplexing trade-off were reported.
2006	Yang and Belfiore [44]	
2007	Yang and Belfiore [45]	A generalized successive relaying protocol was proposed, offering further insights both into the achievable rates and into the associated diversity-multiplexing trade-off. The successive relaying induced interference problem was also mentioned.
	Rankov and Wittneben [34]	
	Fan et al. [46]	
2009	Wicaksana et al. [49]	Techniques for suppressing the successive relaying induced interference were proposed under the idealized assumption that perfect channel state information (CSI) was available at the receiver.
2011	Luo et al. [48]	
	Tian et al. [50]	A sophisticated combination of relay selection, distributed space-time block coding as well as adaptive relaying schemes was proposed for the sake of overcoming the inter-relay interference of the successive relaying regime.

TABLE III
THREE POTENTIAL SOLUTIONS FOR MITIGATING THE 50% THROUGHPUT LOSS INCURRED IN CONVENTIONAL RELAYING PROTOCOLS

Solutions:	Full-Duplex Relaying	Two-Way Relaying	Successive Relaying
Challenges:	Self-Interference	Co-Channel Interference	Inter-Relay Interference
Limitations:	Require infrastructure relays	Limited to bidirectional communications	Require an excessive number of relays

every phase, except for the last phase. Hence, in successive relaying, a normalized throughput of $\frac{L}{L+1}$ is achieved, which will get close to that of direct-transmission upon increasing the number of processing phases L. Consequently, the 50% throughput loss incurred in conventional relaying protocols may be mitigated at the cost of increased delay. The specific actions involved in every phase of Fig. 2 will be further detailed in Section II-A. However, observe in Fig. 2 that increased interference will be encountered both at the RNs and at the DN, which is termed inter-relay interference (IRI) and co-channel interference (CCI), respectively. To combat the successive relaying induced interference, a range of solutions were proposed in [47]–[49]. Furthermore, the authors of [50] replace the repetition of source symbols by the relays as in [46] with a simple coding scheme for the sake of achieving full diversity by using signal space diversity techniques. Further improvements based on space-time block coding combined with coordinate interleaving are derived in [51]. The effect of the successive relaying induced interference will be discussed in detail in Section III-C.

The history of successive relaying is briefly summarized in Table II.

The above-mentioned solutions conceived for recovering the conventional relaying-induced 50% throughput loss are summarized in Table III, where the challenges they have to overcome as well as the constraints they encounter are also highlighted. Instead of assuming a fixed relaying infrastructure based cooperative network, we rely on mobile relays constituted by idle mobile users, which is a more economical approach. Again, the above-mentioned two-way relaying protocol is applicable only to bidirectional communications. By contrast, the successive relaying approach is free from this constraint. Hence successive relaying may be regarded as a more versatile solution provided that its delay is tolerable. ***Hence, in this treatise, we provide a detailed review of and tutorial on the design of successive relaying protocols conceived for recovering the 50% throughput loss of conventional HD relaying***.

Furthermore, we will pay particular attention to the system's coherent versus non-coherent (NC) detection strategy.

Classical coherent detection techniques rely on knowledge of CSI for mitigating the deleterious effects of fading channels. Practical channel estimation techniques typically rely on pilot symbol assisted training techniques [52] and on the fact that in general the consecutive channel impulse response (CIR) taps are correlated in time, as governed by the normalized Doppler frequency. However, an M-transmitter, N-receiver MIMO system has to estimate $(M \times N)$ channels, which will substantially increase the complexity of the entire system, especially at high normalized Doppler frequencies. Furthermore, in the specific scenario of a VAA-assisted cooperative network, it is unrealistic to expect that in addition to the task of relaying, the relay-station would dedicate further precious resources to the estimation of the source-to-relay channel in support of coherent detection. Based on these discussions, NC detection schemes may be deemed to be promising solutions in the context of cooperative networks, since they are capable of retaining the cooperative diversity gain, while circumventing the potentially excessive burden of multiple-antenna based channel estimation.

Numerous differential detection schemes have been devised for noncoherent receivers. For AWGN channels, the conventional differential detection (CDD) philosophy was further developed to multiple-symbol differential detection (MSDD) by Divsalar et al. in [53] for the sake of reducing the BER performance gap between the CDD of M-ary phase-shift keying (MPSK) and the coherent detection of differentially encoded MPSK. This performance gain over CDD is achieved by extending the observation interval from two adjacent symbols to multiple consecutive symbols, while at the same time making a joint decision on these multiple consecutive symbols. A fast algorithm for MSDD was also proposed in [54]. However, the main disadvantage of MSDD is its high complexity. By contrast, Leib et al. [55] and Edbauer [56] proposed simple decision-feedback aided differential detection (DF-DD)

techniques, which achieve an equally competitive performance at a low computational complexity. Later, Adachi *et al.* [57] demonstrated that these DF-DD techniques can be regarded as an approximate realisation of MSDD that proposed by Divsalar *et al.* in [53], which are capable of significantly reduce the computational complexity at the cost of incurring a slight degradation of the BER performance.[3] For fading channels, especially in high-Doppler scenarios, the CDD typically exhibits a high BER-floor. To reduce this error-floor, Divsalar *et al.* [58] and Ho *et al.* [59] further improved the original MSDD algorithm by taking into account the channel's correlation matrix in the multiple-symbol detection metric. Similarly, to mitigate the system's computational complexity, the DF-DD technique was also extended to Rayleigh fading channels in [60]. As a further milestone, the sphere decoding algorithm advocated in [61] was incorporated into the MSDD algorithm of [58] and [59] by Lampe *et al.* in [62], which resulted in the conception of the multiple-symbol differential sphere detection (MSDSD) technique. The MSDSD algorithm substantially reduces the complexity of the MSDD algorithm without any BER degradation with respect to the MSDD algorithm [58]. Hence it achieves a better trade-off between the attainable BER performance and the associated decoding complexity and therefore attracted considerable attention. However, the decoding complexity of the MSDSD algorithm imposed at low SNRs still grows exponentially upon decreasing the SNR. For solving this particular drawback of MSDSD, Pun *et al.* devised the Multiple-Symbol Differential Detection based Fano-algorithm (Fano-MSDD) in [63] and [64] by further developing Fano's original algorithm [65] as an efficient MSDD receiver. On the other hand, to transform the hard-decision-based (HDB) MSDSD algorithm to a more energy-efficient, soft-decision-based (SDB) iterative detection scheme, the MSDSD algorithm was further developed into the soft-input soft-output MSDSD (SISO-MSDSD) regime of [66].

For the sake of supporting the operation of cooperative systems, the noncoherent detection algorithms employed at the DN should become capable of simultaneously processing the multiple input signal sequences received via both the source-to-destination link and the relay-to-destination link. More explicitly, as a benefit of cooperative diversity, the DN of a cooperative network will have to combine multiple versions of the same codeword transmitted via both the source-to-destination link and relay-to-destination links. For the sake of satisfying this requirement, the MSDSD algorithm of [62] was further modified by Wang *et al.* in [67] and [68]. We will refer to this variant of the MSDSD algorithm as the "multiple-path processing based MSDSD". Consequently, the application scenario of the MSDSD algorithm was extended from single-link direct transmission based systems to cooperative systems. Motivated by [67] and [68], the single-user/single-path MSDSD algorithm of [62] was further developed into a novel relay-aided form in [69]. Compared to [67] and [68], the relay-aided MS-DSD scheme of [69] further mitigates the system's complexity and exhibits an increased flexibility in terms of adapting to
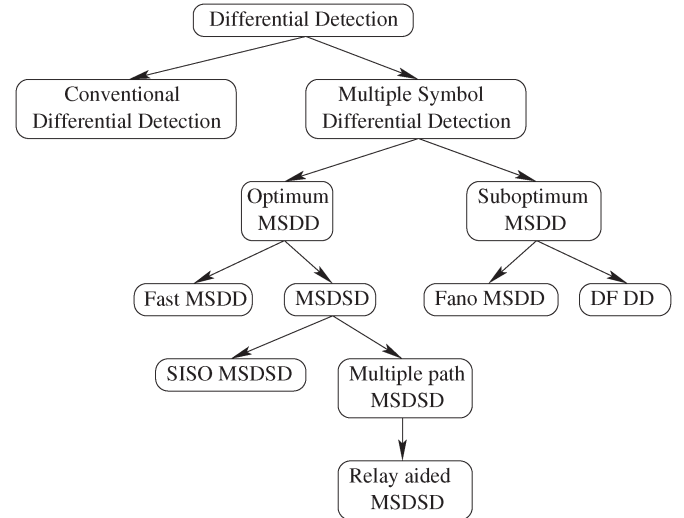

Fig. 3. Evolution of the multiple-symbol differential detectors: CDD [74], MSDD [53], [73], Fast-MSDD [54], DF-DD [57], [60], Fano-MSDD [63], MSDSD [62], SISO-MSDSD [66], Multiple-path MSDSD [67], Relay-aided MSDSD [69], [70].

multi-user, multi-relay scenarios. As a further advance, the soft-decision based version of the relay-aided MSDSD was extended in [70], to create the relay-aided soft-input soft-output MSDSD (relay-aided SISO-MSDSD).

We summarize the above-mentioned history of multiple-symbol differential detection techniques in Table IV. Similar to [71], Fig. 3 is provided for visualizing the evolution of the noncoherent differential detection techniques.

Based on the above brief review of NC detection techniques, in view of their benefits in obviating the need for channel estimation and in overcoming the problem that we cannot expect the mobile relays to estimate the source-to-relay channels, we advocate the family of NC detection techniques, especially the MSDSD algorithms of [62] and [66] as well as their relay-aided MSDSD variants [69], [70] as the detection strategy to be used for successive relaying aided cooperative networking. ***Hence, in the rest of this treatise, we focus our discussions on advanced non-coherent successive relaying (NC-SR).***

A. Outline of the Paper

As addressed early in Section I, to avoid the potential correlation of the antenna elements routinely encountered in conventional MIMO systems, while retaining the spectral efficiency of the multi-antenna systems, the successive relaying aided cooperative network was advocated. Then, for the sake of circumventing the potentially excessive-complexity and hence power-hungry channel estimation, whilst still exhibiting a competitive BER performance, the family of noncoherent differential multiple-symbol joint detection algorithms was investigated in the context of advanced NC-SR regimes. ***Hence, our goal with this review is to stimulate further research and to inspire additional novel contributions on spectrally-efficient cooperative systems dispensing with channel-estimation.***

In our forthcoming discourse, in general, we will portray the historic development of the NC-SR regime from its original

---

[3]Hence, in the perspective of achievable BER performance, we categorize DF-DD into sub-optimum MSDD in Fig. 3.

TABLE IV
CONTRIBUTIONS TO MULTIPLE-SYMBOL DIFFERENTIAL DETECTION

Year	Authors	Contributions
1968	Van Trees [72]	Contributed the critical theoretical foundation of the MSDD algorithm.
1990	Divsalar et al. [53], [73]	Heralded the MSDD algorithm by using a multiple-symbol observation interval during the differential detection process and analysed its BER performance in AWGN channels.
1992	Ho and Fung [59]	Redesigned the decision metric of the MSDD algorithm [53] by introducing the channel's correlation matrix. As a result, the application of the MSDD algorithm was extended to correlated Rayleigh fading channels. The associated BER performance was analysed.
1994	Mackenthun [54]	Developed a fast algorithm for MSDD [53], which imposes a complexity order of only $N \log_2(N)$ per N symbols in AWGN channels.
1999	Schober et al. [60]	Extended the DF-DD algorithm to Rayleigh fading channels, where the per-symbol complexity of the MSDD algorithm grows linearly with the observation window size. Consequently, a sub-optimum trade-off between the performance attained and the complexity imposed was struck.
2005	Lampe et al. [62]	Further developed the MSDD algorithm to the contemporary state-of-the-art noncoherent detection regime - MSDSD.
	Pun and Ho [63]	Proposed the Fano-MSDD algorithm as an alternative technique of MSDSD for low-SNR scenarios.
2006	Pauli et al. [66]	Devised the energy-efficient, soft-decision-aided SISO-MSDSD regime.
2009	Wang and Hanzo [67]	Applied the MSDSD algorithm to cooperative networks, and consequently generated the multiple-path MSDSD.
2011	Li et al. [69], [70]	Created both the hard-decision and soft-decision based relay-aided MSDSD, which was exclusively designed for handling multiple input information streams at the DN of a cooperative network, while dispensing with CSI.

basic representative to its most sophisticated architecture, step by step. In each step, we may introduce a number of basic concepts and principles, portray the system's architecture, identify the fundamental challenges encountered, detail the associated solutions, consider the realistic transceiver design principles, as well as derive a variety of theoretical performance bounds.

In more detail, we will offer further insights into the advantages of the successive relaying (SR) regimes in Section II-A, where the SR regime and other relaying regimes, as well as among different SR regimes are compared. Then, the trade-off between the BER performance gain attained and the complexity imposed by the MSDSD algorithm is characterised in Section II-C, while the mathematical derivation leading from the MSDSD algorithm of [62] to the HDB relay-aided MSDSD and further to the SDB relay-aided MSDSD is provided in Section II-D and E. The design principles of these algorithms are also highlighted. These tutorial components focusing on both the SR regime and on the relay-aided MSDSD algorithm can be regarded as preliminaries for the ensuing discussions of our original contributions.

Consecutively, two prototypes are introduced herein, namely the successive AF relaying aided direct-sequence code-decision multiple-access (DS-CDMA) uplink of Section III and the successive DF relaying aided DS-CDMA uplink of Section IV. In Section III, we move forward from the "single-user" scenario to the "multi-user" scenario. In Section IV, we equip the system with a powerful error correction capability.

Finally, we conclude in Section V. Some potential future research topics in the area of NC-SR are also highlighted in Section V. For the sake of facilitating the readers, the glossary is shown in Table XIV. Hence, the overall structure of this treatise may be summarized as in Fig. 4, in which DCMC is an abbreviation for discrete-input continuous-output memoryless channel.
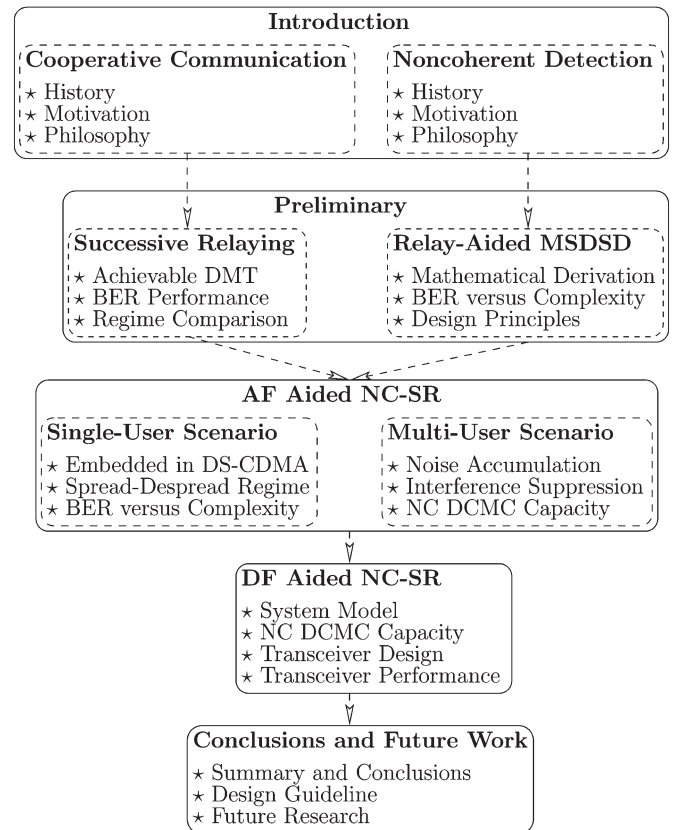

Fig. 4. Outline of the paper.

II. PRELIMINARY: ADVANTAGES OF SR AND THE EMERGENCE OF RELAY-AIDED MSDSD

A. Advantages of Successive Relaying

The transmission schedule of the successive relaying protocol was illustrated in Fig. 2. However, for clarifying it further by
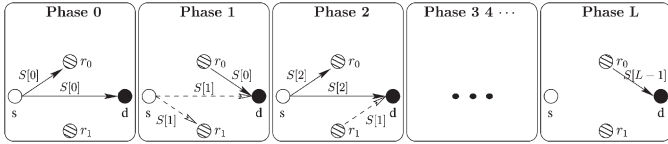
Fig. 5. Simplified transmission schedule of the successive relaying protocol, where the IRI is omitted.

focusing only on the desired signal components whilst ignoring the effects of the IRI, the simplified transmission arrangement of the successive relaying protocol is displayed in Fig. 5. Correspondingly, the specific actions involved in every phase shown in Fig. 5 are described as follows

- **Phase 0**: The SN s broadcasts the message $S[0]$; the RN r_0 listens to the SN s and receives the message $S[0]$; the RN r_1 remains silent; the DN d receives the message $S[0]$.
- **Phase 1**: The SN s continues to broadcast the message $S[1]$; the RN r_0 forwards the message $S[0]$ to the DN; the RN r_1 listens to the SN s and receives the message $S[1]$; the DN d simultaneously receives the messages $S[0]$ and $S[1]$ via the relay-to-destination link and source-to-destination link, respectively.
- **Phase 2**: The SN s continues to broadcast the message $S[2]$; the RN r_0 listens to the SN s and receives the message $S[2]$; the RN r_1 forwards the message $S[1]$ to the DN; the DN d simultaneously receives the messages $S[1]$ and $S[2]$.
- **Phase 3 4 $\cdots$**: The transmission options described in Phase 1 and 2 will be alternately repeated until Phase $(L-1)$.
- **Phase L**: The SN s completes all of its transmissions and stops broadcasting; the RN r_0 or r_1 forwards the message $S[L-1]$ to the DN; another RN remains silent; the DN d receives the message $S[L-1]$.

As mentioned earlier, Fan *et al.* [46] analysed the DMT[4] of DF based successive relaying, while assuming perfect source-to-relay links. The algebraic relationship between the diversity order and the associated multiplexing gain was also formulated by them in [46, (33)]. Based on [46, (33)], the DMT struck by successive DF relaying relying on L processing phases is depicted in Fig. 6. The DMTs achieved by direct transmission, conventional DF relaying, as well as conventional AF relaying are also shown in Fig. 6 as the benchmarks, which are directly abstracted from [11, Fig. 6]. As argued before, successive DF relaying is capable of achieving a significantly improved DMT compared to conventional DF or AF relaying. This specific benefit of successive relaying is evidenced again in Fig. 6.

For the sake of extending our horizon further as well as of further manifesting the advantage of SR, we would like to compare several typical relaying regimes herein, which include full-duplex relaying (FDR), SR, two HD relays aided

---

[4]In general, a MIMO system (including cooperative systems) can provide two types of gains: diversity gain and multiplexing gain. However, maximizing one type of gain may not necessarily maximize the other. To compare the performance between diversity-oriented and multiplexing-oriented schemes, Zheng and Tse defined the concept of DMT $D(r)$ in [5], which represents the diversity order D as a function of the multiplexing gain r. The DMT is essentially the trade-off between the error probability and the data rate of a system.
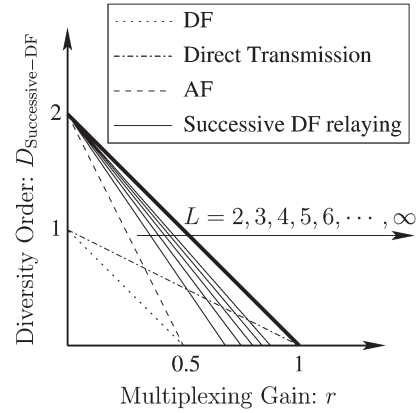

Fig. 6. Diversity order versus multiplexing gain r for the successive DF relaying protocol, where the number of processing phases L is increased from $L = 2$ to ∞. The relevant curves are attained according to [46, (33)]. Then, according to the transmission process depicted in Fig. 5, intuitively, the normalized throughput of successive DF relaying (or its multiplexing gain) is limited to the region of $r \in \left[0, \frac{L}{L+1}\right]$. The DMT of both the conventional DF relaying and of the AF relaying as portrayed in [11, Figure 6] are also included here as a pair of benchmarks.
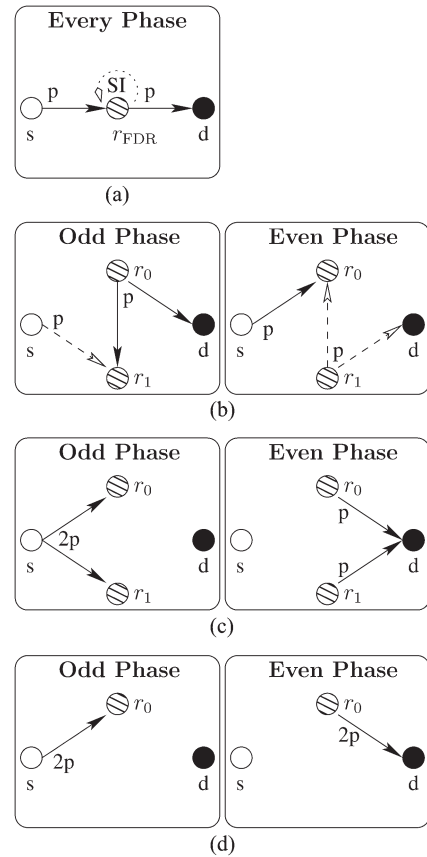

Fig. 7. Transmission framework of a range of typical relaying regimes. The detailed interpretation of each regime can be found in Table V. (a) Full duplex relaying. (b) Successive relaying. (c) Two HD relays aided CR. (d) Single HD relay aided CR.

conventional relaying (CR), as well as a single HD relay aided CR. Their transmission frameworks are compactly illustrated in Fig. 7 and the associated interpretations can be found in Table V. For the sake of a fair comparison, the transmit power of all the competitive relaying regimes is fixed to $2P$. For example,

TABLE V
DETAILED INTERPRETATIONS OF THE RELAYING REGIMES INVOLVED IN FIG. 7

|	
full-duplex relaying (FDR)	A full-duplex relay node is employed, which is capable of transmitting and receiving signals simultaneously. Hence the SN-to-RN and the RN-to-DN transmissions can be completed in a single phase.
successive relaying (SR)	Relying on a large number of processing phase of L, we can only utilize the "Phase 1" and "Phase 2" in Figure 2 to summarize the entire transmission arrangement of SR. If we further ignore the direct SN-to-DN link owing to its large distance, we obtain "(b) successive relaying" in Figure 7.
two HD relays aided CR	During the broadcast phase, the SN s broadcast its information, while two RNs r_0, r_1 listen to the SN. During the cooperative phase, two RNs r_0, r_1 simultaneously forward the SN's information heard in the last phase to the DN.
single HD relay aided CR	It is the fundamental relaying prototype and has a similar transmission arrangement to that of "(c) two HD relays aided CR". By contrast, instead of exploiting multiple RNs, it only employs a single HD RN.
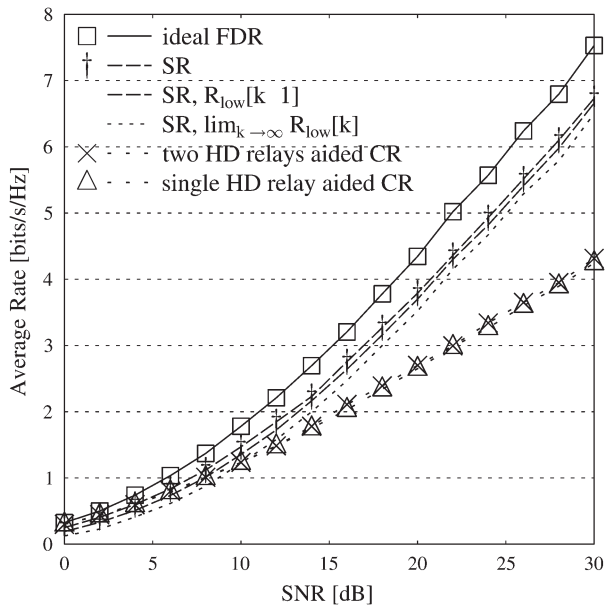
Fig. 8. Performance of several relaying schemes in terms of average achievable error-free data rate versus SNR. All the competitive relaying regimes employ AF relaying protocol. Particularly, it is assumed that the SI incurred in the "full-duplex relaying" of Fig. 7(a) has been perfectly cancelled, which results in the curve marked "ideal FDR" in this figure. Then, the strength of IRI incurred in SR is assumed to be the half of the desired signals. These simulation results are based on [34] and they can also be found in [34, Fig. 6].

485 since there are always two transmitters in every phase of "(b)
486 successive relaying", both the SN s and the RN $r_i, i \in 0, 1$
487 transmit their signals at the power of P. By contrast, in each
488 phase of "(d) single HD relay aided CR", there is only a single
489 transmitter. Hence, either the SN s or the RN r_0 transmits
490 signals at the power of $2P$. Furthermore, it is assumed that
491 the direct Source-to-Destination link is negligible owing to the
492 associated large propagation distance.
493   Consequently, the average achievable error-free data rate
494 versus SNR performance of each relaying regime of Fig. 7 is
495 shown in Fig. 8, where all the cooperative regimes employ
496 the AF relaying protocol. In [34], three different regimes were
497 considered, namely the SR regime employing adaptive rate
498 allocation, the SR regime transmitting exactly at the ergodic
499 capacity of time slot $[k + 1]$ as the fixed transmit rate of its
500 SN, as well as the SR regime transmitting at the ergodic
501 capacity of time slot $k \to \infty$ as the fixed transmit rate of its

SN. They are denoted by "SR", "SR, $R_{\text{low}}[k + 1]$", and "SR, 502
$\lim_{k \to \infty} R_{\text{low}}[k]$" in Fig. 8, respectively. Observe in Fig. 8 that 503
replacing adaptive rate allocation by the fixed rate allocation 504
scheme will sightly degrade the performance of SR. Neverthe- 505
less, the performance of these SR regimes is still close to that 506
of the "ideal FDR". Furthermore, they significantly exceed the 507
performance of the "single HD relay aided CR" or of the "two 508
HD relays aided CR" beyond SNR = 10 dB. More particularly, 509
observe in Fig. 7 that both the "(b) successive relaying" and 510
the "(c) two HD relays aided CR" require an identical number 511
of RNs. However, the SR regime is capable of substantially 512
outperforming its conventional relaying based counterpart. This 513
fact underlines the advantage of the SR regime. 514
   Furthermore, depending on the specific type of protocol 515
employed at the RN, the SR regime illustrated in Fig. 7 can be 516
categorised into AF aided SR and DF aided SR. The AF aided 517
SR regime has been investigated in Fig. 8. Then, according to 518
whether the RNs do or do not invoke IRI cancellation, the DF 519
aided SR can be further categorised into two types, namely the 520
"DF aided SR, where the RNs dispense with IRI canc." and the 521
"DF aided SR, where the RNs employ IRI canc.". Hence, it is 522
worth providing further insights into SR by comparing these 523
different SR regimes. As revealed in [34], the performance of 524
these different SR regimes is predetermined by their ability to 525
mitigate the IRI effects. Hence it is insightful to compare their 526
error-free data rates versus the IRI power, which are shown 527
in Fig. 9, where the "ideal DF aided FDR" system is similar 528
to the "ideal FDR" system shown in Fig. 8, but with its AF 529
protocol employed at the FD relay replaced by the DF protocol. 530
Then, the "AF aided SR, DN employs IRI canc." system of 531
Fig. 9 is the same as the system, namely "SR" in Fig. 8. 532
Furthermore, the "single HD-DF relay aided CR" system of 533
Fig. 9 is obtained upon replacing the AF protocol employed 534
by the "single HD relay aided CR" system in Fig. 8, by the DF 535
protocol. Furthermore, the IRI to signal power ratio (ISR) is 536
used as the horizontal axis in Fig. 9. 537
   Observe in Fig. 9 that for ISR ≥ 10 dB, the RNs of the SR 538
system should perform the IRI cancellation before detecting the 539
messages transmitted by the SN. Specifically, it is beneficial 540
to invoke the regime, namely "DF aided SR, RNs employ IRI 541
canc.". By contrast, if the IRI is sufficiently weak, e.g. when 542
we have ISR ≤ −15 dB, it is not necessary to invoke IRI 543
cancellation at the RNs of the SR system. Instead, it is better 544
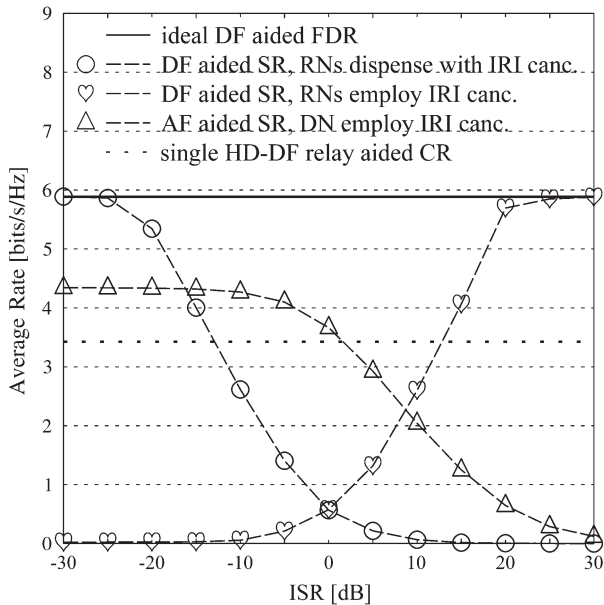to directly decode the signals transmitted by the SN at the RNs 545

Fig. 9. Comparison among different SR regimes in terms of their average achievable error-free data rates versus ISR. The signal to noise power ratio of the desired signal is fixed to SNR = 20 dB. These simulation results are based on [34] and they can also be found in [34, Fig. 9].

of the SR system, while considering the IRI to be an additional noise component. Hence, in this case, we may advocate the "DF aided SR, RNs dispense with IRI canc." regime. In the case of incurring weak or moderate IRI, for example, when we have ISR $\in (-15, 10)$ dB, we may opt for the AF aided SR regime. Since our DS-CDMA based interference suppression technique, which will be introduced in Section III-A and C2 is capable of sufficiently suppressing the IRI. Generally, in Sections III and IV, we operate the SR systems in weak IRI scenarios. Hence, we may focus our attention on AF aided SR, as well as on DF aided SR, where the RNs directly decode the signals transmitted by the SN, while regarding the IRI as an additional noise component.

B. Precondition of Embedding Successive Relaying Into DS-CDMA System

As summarized in Table III, SR imposes both co-channel interference and inter-relay interference at the DN. These SR induced interferences may significantly degrade the benefits of the SR [34], [46].

Against this background, we invoked the DS-CDMA technique in [75] and designed the successive relaying aided cooperative DS-CDMA uplink. In this transmission framework, the successive relaying aided network (SRAN) is embedded in the DS-CDMA uplink for improving the communication quality of a cell-edge user. Hence, the DS-CDMA technique is used for mitigating the successive relaying induced interference between the transmitted signals of the source and relay.

In more detail, for the sake of a fair comparison to the conventional two-phase cooperative system [11], we have to ensure that no extra channel resources are required by the advocated successive relaying aided cooperative DS-CDMA

TABLE VI
SYSTEM PARAMETERS EMPLOYED IN FIGS. 11 AND 12   AQ2

Scenario	Depicted in Figure 10
Channel Model	Narrow-Band Flat-Fading Channel
Normalized Doppler Frequency	$f_d = 0.03$
Modulation	4-PSK for Coherent Detection 4-DPSK for Differential Detection
Detector	Coherent Detector Coherent Differential Detector NC Differential Detector SL MSDSD (or MSDD)
Window Size of MSDSD	$N = 6, 10$

uplink. Practically, governed by a certain target BER value, there may be a strict limit on the number of active users that can be supported in a DS-CDMA system, which we denote by "$U_{\text{Threshold}}$". In general, it is realistic to assume that there are some idle users in a DS-CDMA cellular system. Hence, the preconditions of employing the SRAN in support of a cell-edge user in the DS-CDMA system may be as follows:

1. We find a sufficient number of idle users between the SN and DN, willing to support the cell-edge user.
2. The sum of the number of active users and relays, namely $U_{\text{ACT}} + U_{\text{RN}}$ is still lower than $U_{\text{Threshold}}$.

In other words, the relays employed in the SRAN are the idle users of the DS-CDMA cellular system. Moreover, since we assume that $U_{\text{ACT}} + U_{\text{RN}} < U_{\text{Threshold}}$, the system does not run out of spreading sequences. However, appointing idle users to serve as the relays increases the total number of active entities in the DS-CDMA cellular system, hence increasing the interference. Therefore, it may be concluded that the proposed successive relaying aided cooperative DS-CDMA uplink essentially converts the typical 50% half-duplex relaying-induced throughput loss to a potential user-load reduction of the CDMA system.

C. MSDSD: Improving the Trade-Off Between the Power Gain and Decoding Complexity

As stated early in Section I, CDD will exhibit a high error-floor in fading scenarios. This is demonstrated in Fig. 11 by the dashed curve marked by the heart legends, where a flat Rayleigh fading channel having a normalized Doppler frequency of $f_d = 0.03$ was considered. As summarized in Table IV, for the sake of accommodating fading channels, Ho *et al.* [59] as well as Divsalar *et al.* [58] introduced the channel correlation matrix into the initial MSDD algorithm proposed by Divsalar *et al.* in [53]. By exploiting both the increased time-diversity gain of the extended observation window size and the statistical knowledge of the channel, the BER performance of the improved MSDD algorithm [58], [59] is capable of approaching the lower bound of differential detection, namely that achieved by coherent differential detection. The beneficial effect of increasing the observation window size is demonstrated by the solid lines in Fig. 11.

However, when employing M_c-ary differential phase-shift keying (M_c-DPSK) and an observation window size of N, to make a decision concerning the differential symbol sequence **S** transmitted during an observation window, the MSDD
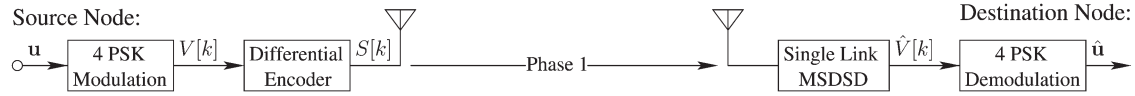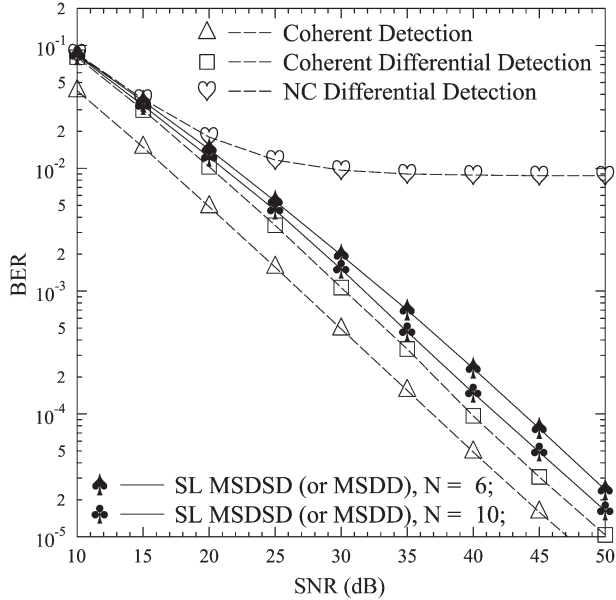
Fig. 10.   Schematic of single-link MSDSD.

Fig. 11.   BER performance of the single-link (SL) direct-transmission (DT) based MSDSD (or MSDD) when encountering a flat Rayleigh fading channel having a normalized Doppler frequency of $f_d = 0.03$ and employing 4-DPSK modulation. The associated BER performance of coherent detection, coherent differential detection, and conventional differential detection are also portrayed. The results for SL MSDSD (or MSDD) are based on the schematic of Fig. 10.
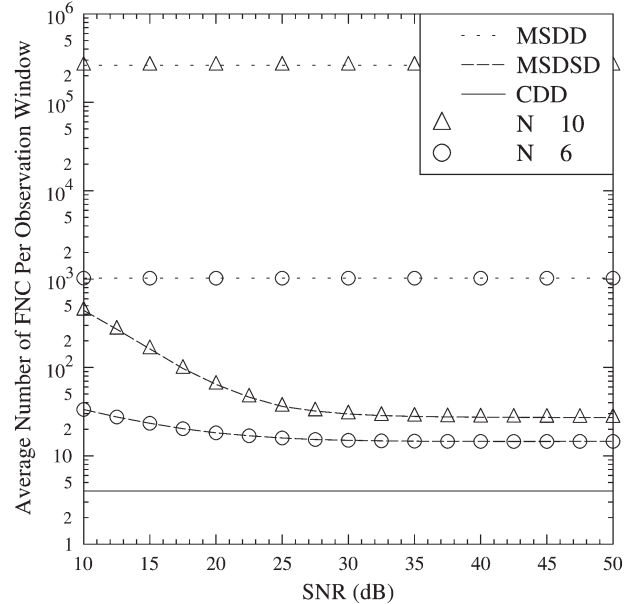
Fig. 12.   The decoding complexities associated with the CDD, MSDSD and MSDD schemes employed in Fig. 11 are compared here, where the average number of FNCs required for decoding a single observation interval is employed as the complexity metric. The results are based on the schematic of Fig. 10 as well as on the parameters of Table VI.

algorithm has to test all of its M_c^{N-1} legitimate combinations.[5] In more detail, each Frobenius norm,[6] which is determined by both a specific legitimate combination of **S** and the actual received signal sequence is calculated. Then, the particular legitimate combination of **S**, which results in the minimum Frobenius norm is deemed to be the optimum decision. We may refer to Fig. 16, which visualizes the search space of the MS-DSD algorithm [62], as will be discussed later in Section II-D for the sake of capturing the philosophy of this detection process. Hence, the Frobenius norm calculation (FNC) constitutes the major contribution of the system's decoding complexity. Accordingly, the average number of FNCs required for decoding a single differential symbol sequence **S** can be employed as a basic metric for evaluating the decoding complexity of the multiple symbol joint detection based algorithms, such as MSDD and the MSDSD.[7]

In this spirit, the MSDD algorithm imposes a decoding complexity of M_c^{N-1} FNCs per observation window. By contrast, the CDD algorithm only requires M_c FNCs per observation window. Hence, the power gain of the MSDD algorithm with respect to the CDD algorithm as shown in Fig. 11 is obtained at the cost of imposing a significantly higher decoding complexity. Therefore, an improvement of the trade-off between the power gain obtained and the associated decoding complexity was desired. With this objective, Lampe *et al.* [62] devised the powerful MSDSD algorithm, which is capable of excluding some legitimate combinations of **S** from the search space without going all the way to completing their associated FNCs. As a benefit, the brute-force maximum-likelihood search involved in the MSDD algorithm is obviated without sacrificing the attainable BER performance. This decoding complexity reduction facilitated by the MSDSD algorithm is demonstrated in Fig. 12. Based on Figs. 11 and 12, the MSDSD algorithm significantly reduces the decoding complexity of the MSDD algorithm, while retaining its BER performance. Hence the compromise between the power gain obtained and the associated decoding complexity of the NC detection techniques is improved.

To further improve the trade-off between the power gain achieved and the decoding complexity of NC detection, the single-path MSDSD algorithm of [62] was further developed into a novel multiple-path form in [67] and [68], where the original MSDSD algorithm was appropriately modified and applied to cooperative systems. For example, the schematics of the cooperative systems relying on the "twin-path" MSDSD and on the "triple-path" MSDSD are portrayed in Figs. 13 and 14, respectively.

---

[5]As a reference symbol, the last differential symbol of an observation interval is always fixed, which therefore does not require any detection.

[6]Its precise definition is given in (4) of Section II-D.

[7]The complexity imposed by the sorting operation during the differential decoding process of MSDSD may be ignored for the sake of simplifying the complexity comparison among CDD, MSDD and MSDSD.
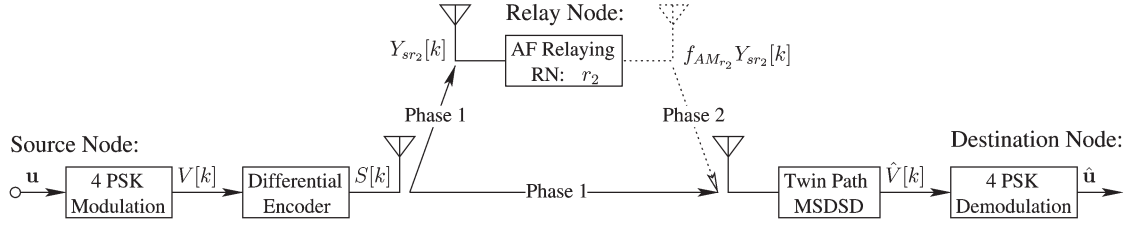
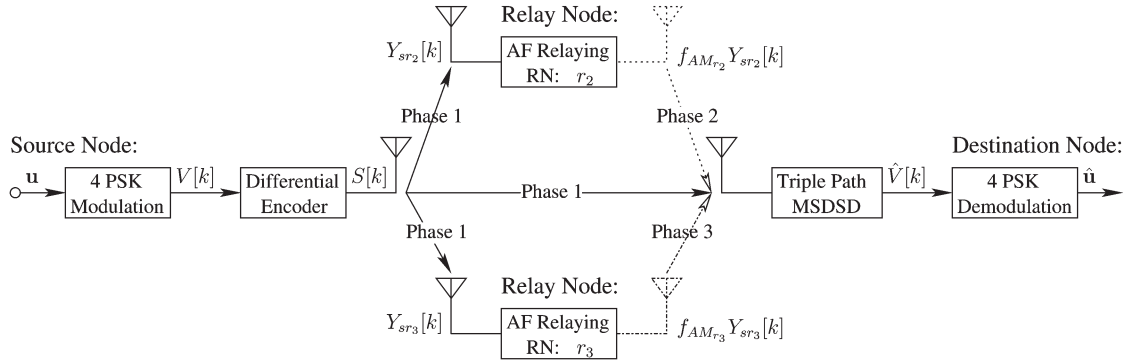Fig. 13. Schematic of twin-path MSDSD based AF relaying.

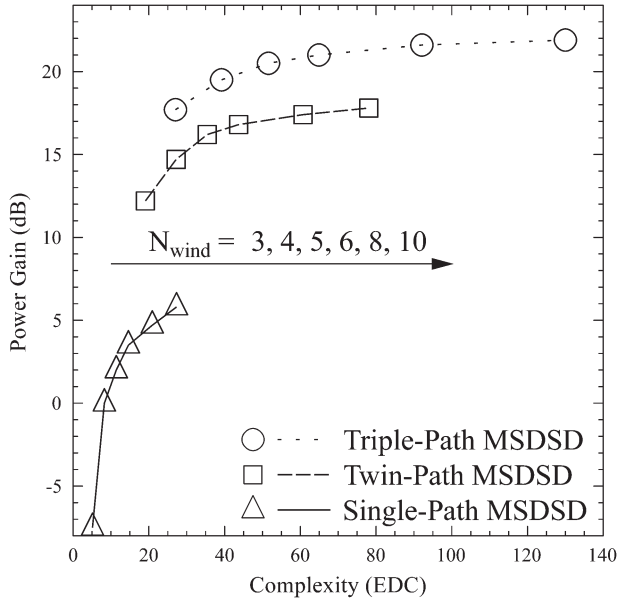Fig. 14. Schematic of triple-path MSDSD based AF relaying.

Fig. 15. Power gain versus complexity for single- and multiple-path MSDSD, where the power gain is expressed in terms of the SNR. Then, the SNR required by the single-path MSDSD algorithm having an observation window size of $N_{\text{wind}} = 4$ for approaching the target BER of 10^{-4} when encountering a flat Rayleigh fading channel having $f_d = 0.03$ is regarded as the power-gain benchmark. The results of the "single-path" system, the "twin-path" system and the "triple-path" system are based on the schematics of Figs. 10, 13, and 14, respectively, where all the parameters employed are summarized in Table VII.

TABLE VII
SYSTEM PARAMETERS EMPLOYED IN FIG. 15   AQ3

Scenario	Depicted in Figures 10, 13 and 14
Channel Model	Narrow-Band Flat-Fading Channel
Normalized Doppler Frequency	$f_d = 0.03$
Modulation	Differential QPSK
Detector	Single-Path MSDSD Twin-Path MSDSD Triple-Path MSDSD
Window Size of MSDSD	$N \in \{3, 4, 5, 6, 8, 10\}$

However, as commented in Section I, as well as shown in Table IV, the multiple-path MSDSD [67], [68] remains insufficiently flexible for application in cooperative networks, especially when having a large number of propagation paths in the cooperative network owing to employing multiple RNs. Correspondingly, the relay-aided MSDSD of [69] and [70] was devised, which can be readily applied to various cooperative networks having an arbitrary number of RN induced propagation paths. This is achieved without any BER performance degradation with respect to multiple-path MSDSD [67], [68]. The conception of both the HDB and the SDB relay-aided MSDSD is briefly highlighted in Section II-D and E.

D. HDB Relay-Aided MSDSD

Let $\mathbf{V}$ denote an information symbol vector, which consists of $(N - 1)$ M_c-ary PSK information symbols $V[k] \in \{e^{j2\pi m/M_c}; m = 0, 1, \cdots, M_c - 1\}$. Then, $\mathbf{V}$ is differentially encoded to a DPSK symbol vector $\mathbf{S}$ having a length of N. After $\mathbf{S}$ is transmitted from uth entity (SN or RN) to the DN via a flat Rayleigh fading channel having a CIR vector of $\mathbf{H}_u$, the differential decoder in Fig. 10 will receive a signal vector $\mathbf{Z}_u$, which is a distorted version of $\mathbf{S}$. Hence we have the following relationships: $\mathbf{V} = [V[1], V[2], \ldots, V[N-1]]^T$, $\mathbf{S} = [S[1], S[2],$

The relevant improvement of the trade-off between the power gain attained and the associated decoding complexity is revealed in Fig. 15, where the SNR required by the single-path MSDSD algorithm having observation window size of $N_{\text{wind}} = 4$ for approaching the target BER of 10^{-4} when encountering a flat Rayleigh fading channel having $f_d = 0.03$ is regarded as our power-gain benchmark.

$\dots, S[N]]^T$, $\mathbf{H}_u = [h_u[1], h_u[2], \dots, h_u[N]]^T$, $\mathbf{Z}_u = [z_u[1],$ $z_u[2], \dots, z_u[N]]^T$, $\mathbf{N} = [N[1], N[2], \dots, N[N]]^T$ and

$$S[k+1] = S[k]V[k],$$
$$\mathbf{Z}_u = \mathbf{H}_u \circ \mathbf{S} + \mathbf{N}, \tag{1}$$

where $\circ$ denotes the Hadamard product, and we have $N[k] \sim \mathcal{CN}(0, \sigma^2)$.

Obviously, there are $(M_c)^{N-1}$ legitimate combinations of the information symbol vector $\mathbf{V}$, which may be denoted by the set χ. Hence the challenge encountered by the noncoherent differential multiple-symbol joint decoder is that of finding the actually transmitted information vector $\mathbf{V}$ out of the entire set χ, when relying only on the received signal vector $\mathbf{Z}_u$. The mathematical principle behind this problem relates to the so-called "general Gaussian problem" [72].

Based on [72] and Divsalar's original MSDD algorithm [53], Ho and Fund [59] rewrote the specific form of the conditional probability density function (PDF) of the received signal vector $\mathbf{Z}_u$, conditioned on the transmitted DPSK symbol vector $\mathbf{S}$, which may be formulated as

$$\Pr(\mathbf{Z}_u | \mathbf{S}) = \frac{1}{(2\pi)^{\frac{N}{2}} \|\mathbf{\Phi}_{\mathbf{Z}_u \mathbf{z}_u}\|^{\frac{1}{2}}} \exp\left(-\frac{1}{2} \mathbf{Z}_u^H \mathbf{\Phi}_{\mathbf{Z}_u \mathbf{z}_u}^{-1} \mathbf{Z}_u\right), \tag{2}$$

where the correlation matrix is given by $\mathbf{\Phi}_{\mathbf{Z}_u \mathbf{z}_u} \triangleq \mathrm{diag}\{\mathbf{S}\} \{\mathcal{E}\{\mathbf{H}_u \mathbf{H}_u^H\} + \sigma_n^2 \mathbf{I}_N\} \mathrm{diag}\{\mathbf{S}^*\}$, $\mathbf{I}_N$ is an N-dimensional identity matrix and $\sigma_n^2 = N_0$ is the noise variance.

Accordingly, the previously mentioned challenge encountered by the noncoherent differential multiple-symbol joint decoder can be tackled by selecting the optimum DPSK symbol vector $\hat{\mathbf{S}}$ out of all the $(M_c)^{N-1}$ legitimate candidate vectors, which maximizes the conditional PDF presented in (2). Then, the benefit of presenting the conditional PDF $\Pr(\mathbf{Z}_u | \mathbf{S})$ in the form of (2) is that when the amplitude of any legitimate DPSK symbol $S[k]$ is fixed to unity, the determinant $\|\mathbf{\Phi}_{\mathbf{Z}_u \mathbf{z}_u}\|$ in (2) becomes independent of the DPSK symbol vector $\mathbf{S}$. Hence, when comparing the values of the conditional PDF corresponding to different DPSK symbol vectors, we only have to concentrate our attention on the $(\mathbf{Z}_u^H \mathbf{\Phi}_{\mathbf{Z}_u \mathbf{z}_u}^{-1} \mathbf{Z}_u)$ part on the right hand side of (2). Since the conditional PDF $\Pr(\mathbf{Z}_u | \mathbf{S})$ in (2) is a monotonically decreasing function of the metric $(\mathbf{Z}_u^H \mathbf{\Phi}_{\mathbf{Z}_u \mathbf{z}_u}^{-1} \mathbf{Z}_u)$, maximising $\Pr(\mathbf{Z}_u | \mathbf{S})$ over the entire set of $\mathbf{S}$ is equivalent to minimising $(\mathbf{Z}_u^H \mathbf{\Phi}_{\mathbf{Z}_u \mathbf{z}_u}^{-1} \mathbf{Z}_u)$ over the entire set of $\mathbf{S}$. Hence, the decision rule is simplified to

$$\hat{\mathbf{S}} = \arg\min_{\mathbf{S} \in \chi} \left\{ \mathbf{Z}_u^H \mathbf{\Phi}_{\mathbf{Z}_u \mathbf{z}_u}^{-1} \mathbf{Z}_u \right\}. \tag{3}$$

However, according to the decision rule (3), the minimum decision metric $(\mathbf{Z}_u^H \mathbf{\Phi}_{\mathbf{Z}_u \mathbf{z}_u}^{-1} \mathbf{Z}_u)$ can only be determined, if all the $(M_c)^{N-1}$ legitimate combinations of the DPSK symbol vector $\mathbf{S}$ are substituted into (3) and evaluated. To mitigate this brute-force search problem incurred by the MSDD algorithms of [53] and [59], Lampe *et al.* [62] devised the state-of-the-art NC detection philosophy termed the MSDSD. In [62], the refined decision rule proposed by Ho and Fund [59] and

formulated in (3) may be expressed after a range of algebraic manipulations as

$$\hat{\mathbf{S}} = \arg\min_{\mathbf{S} \in \chi} \left\{ \|\mathbf{U}^u \mathbf{S}\|^2 \right\}, \tag{4}$$

where, the notation $\|\cdot\|$ denotes the Frobenius norm, $\mathbf{U}^u \triangleq (\mathbf{F} \mathrm{diag}\{\mathbf{Z}_u\})^*$, $\mathbf{U}^u \in \mathbb{C}^{N \times N}$, and $\mathbf{F}$ is a triangular matrix, defined via $\mathbf{C}^{-1} = \mathbf{F}^H \mathbf{F}$, where $\mathbf{C} \triangleq \mathcal{E}\{\mathbf{H}_u \mathbf{H}_u^H\} + \sigma_n^2 \mathbf{I}_N$.

The benefit of presenting the multiple-symbol differential decision rule in the form of (4) is that the MSDD algorithm now can be regarded as a "shortest vector problem", which may be efficiently solved by sphere detection [61], [76].

According to the sphere decoding strategy [76], the specific DPSK symbol vectors $\hat{\mathbf{S}}$, which are located within a sphere of radius R, for which we have $\|\mathbf{U}^u \hat{\mathbf{S}}\|^2 \leq R^2$ will be temporarily regarded as potential candidates. Then, the squared Frobenius norm $\|\mathbf{U}^u \hat{\mathbf{S}}\|^2$ will be employed as the new sphere radius. Hence the sphere radius R is further reduced. By contrast, any DPSK symbol vector $\hat{\mathbf{S}}$ that violates the condition of $\|\mathbf{U}^u \hat{\mathbf{S}}\|^2 \leq R^2$ will be excluded from the search. This test is repeated along with a gradually reduced sphere radius R, until only the optimum candidate vector $\hat{\mathbf{S}}$ lies within the sphere. This process is exemplified in Fig. 16, where an observation window of $N = 5$ and a differentially-encoded 4-DPSK differential-detection aided modulation scheme are employed.

Since the matrix $\mathbf{U}^u$ involved in (4) has an upper triangular form, we may carry out the sphere decoding in a component-wise manner. Bearing in mind that we have $\hat{\mathbf{S}} = [\hat{S}[1], \hat{S}[2], \dots, \hat{S}[N]]^T$, the squared Frobenius norm accounting only for the last $(N-i+1)$ components of $\hat{\mathbf{S}}$, i.e. $[\hat{S}[i], \hat{S}[i+1], \dots, \hat{S}[N]]^T$ is a fraction of the total squared Frobenius norm $\|\mathbf{U}^u \hat{\mathbf{S}}\|^2$ in (4). Therefore, once the partial squared Frobenius norm of a legitimate DPSK symbol vector $\hat{\mathbf{S}}$ has already exceeded the current sphere radius R_{current}^2, it is logical that regardless of the first $(i-1)$ components of $\hat{\mathbf{S}}$, i.e. regardless of $[\hat{S}[1], \hat{S}[2], \cdots, \hat{S}[i-1]]^T$, its completed squared Frobenius norm $\|\mathbf{U}^u \hat{\mathbf{S}}\|^2$ must also exceed the current sphere radius R_{current}^2. This implies that $M_c^{(i-1)}$ legitimate combinations of $\hat{\mathbf{S}}$ are justifiably excluded from the search space even without completing their associated FNCs. Consequently, the "Excluded Groups" displayed in Fig. 16 are identified. This is also the major reason why the MSDSD algorithm is capable of significantly mitigating the decoding complexity of the MSDD algorithm, as demonstrated in Fig. 12 of Section II-C.

As mentioned in Section I and detailed in [67] and [68], the MSDSD algorithm formulated in (4) has also been applied in cooperative communication scenarios. One of the critical design issues elaborated on in [67] and [68] is that of combining the multiple relay-aided received signals $\{\mathbf{Z}_u\}_{u=1}^U$, which correspond to the same source symbol sequence, but are transmitted by U users acting as RNs and experiencing different channels. This problem was solved by Wang *et al.* [68] leading to their multiple-path MSDSD algorithm. However, the size of the critical matrix $\mathbf{U}$ of [68, (26)] rapidly increases with the number of multipath components U; hence the implementation of sphere detection based on the decision metric proposed in [68, (26)] becomes a challenge, when the number of multipath
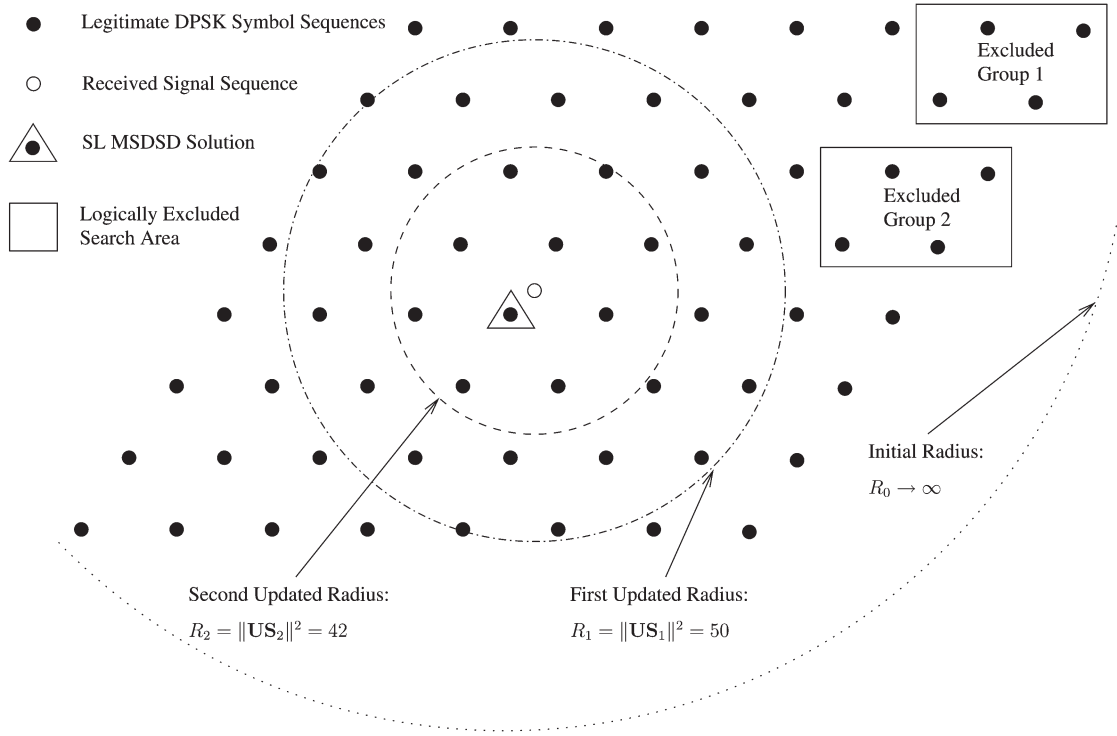
Fig. 16. Search space of the single-path MSDSD. Since we have $N = 5$, there are $M_c^{N-1} = 4^4 = 256$ legitimate DPSK symbol sequence $\hat{\mathbf{S}}$, but to avoid obfuscating details, we only depict part of them, which are explicitly labelled by 64 black dots. Then, the original signal sequence $\mathbf{S}$ will incur an amplitude attenuation and phase rotation of its component 4-DPSK symbols. Hence the received signal sequence represented by the hollow circle in the centre cannot fall onto any of the legitimate DPSK symbol sequences. Instead, it has a certain distance from the black dots. Thus, our MSDSD algorithm aims at finding the black dot that has the minimum distance from the hollow circle, which is deemed to be the original signal sequence $\mathbf{S}$.

U increases. Thus, a new HDB relay-aided MSDSD algorithm was devised in [69].

Since the received sequences $\{\mathbf{Z}_u\}_{u=1}^{U}$ are independent Gaussian random vectors, the corresponding conditional PDF can be written as

$$\Pr\left(\{\mathbf{Z}_u\}_{u=1}^{U}|\mathbf{S}\right) = \prod_{u=1}^{U} \Pr(\mathbf{Z}_u|\mathbf{S}). \tag{5}$$

Upon substituting (2) into (5), (5) may be rewritten as

$$\Pr\left(\{\mathbf{Z}_u\}_{u=1}^{U}|\mathbf{S}\right) = \left(\prod_{u=1}^{U} \eta_u\right) \times \exp\left(-\frac{1}{2}\sum_{u=1}^{U} \mathbf{Z}_u{}^{H}\boldsymbol{\Phi}_{\mathbf{Z}_u\mathbf{Z}_u}^{-1}\mathbf{Z}_u\right), \quad (6)$$

where the factor $\prod_{u=1}^{U}\eta_u$ is independent of $\mathbf{S}$. Hence, the relay-aided MSDSD decision rule of finding the specific sequence $\hat{\mathbf{S}} = [\hat{S}[1], \hat{S}[2], \ldots, \hat{S}[N]]^T$ which maximises the conditional PDF of (6) is equivalent to selecting the particular transmitted source signal sequence $\hat{\mathbf{S}}$, whose matrix sum is the smallest, which is formulated as

$$\begin{aligned}\hat{\mathbf{S}} &= \arg\min_{\mathbf{S}\in\chi}\left\{\sum_{u=1}^{U} \mathbf{Z}_u{}^{H}\boldsymbol{\Phi}_{\mathbf{Z}_u\mathbf{Z}_u}^{-1}\mathbf{Z}_u\right\}, \\ &= \arg\min_{\mathbf{S}\in\chi}\left\{\sum_{u=1}^{U} \|\mathbf{U}^u\mathbf{S}\|^2\right\}. \end{aligned} \tag{7}$$

Then, we further define a $(UN \times N)$-element matrix $\mathbf{U}$ as

$$\mathbf{U} = \begin{bmatrix} \mathbf{U}_{1,1} & \mathbf{U}_{1,2} & \cdots & \mathbf{U}_{1,N} \\ 0 & \mathbf{U}_{2,2} & \cdots & \mathbf{U}_{2,N} \\ \vdots & \vdots & \ddots & \vdots \\ 0 & 0 & \cdots & \mathbf{U}_{N,N} \end{bmatrix}_{UN\times N},$$
$$\mathbf{U}_{i,j} = \left[\mathbf{U}_{i,j}^1, \mathbf{U}_{i,j}^2, \cdots, \mathbf{U}_{i,j}^U\right]^T, \tag{8}$$

where $\mathbf{U}_{i,j}$ is the specific vector component of $\mathbf{U}$ in row i and column j, $1 \le i, j \le N$, and $\mathbf{U}_{i,j}^u$ is a specific element of $\mathbf{U}^u$ in row i and column j, $1 \le i, j \le N$, which was defined in (4). Upon substituting (8) into (7), we finally arrive at the HDB relay-aided MSDSD decision rule

$$\hat{\mathbf{S}} = \arg\min_{\mathbf{S}\in\chi}\left\{\|\mathbf{U}\mathbf{S}\|^2\right\}. \tag{9}$$

The size of the corresponding matrix $\mathbf{U}$ used in [68, (26)] is $(UN \times U^2N)$, which is cubically proportional to the number of entities U. By contrast, the size of the newly devised matrix $\mathbf{U}$ defined in (8) and involved in (9) is reduced to $(UN \times N)$, which only increases linearly with U. Thus, the HDB relay-aided MSDSD algorithm may be decomposed into two steps: first, we individually calculate each $\mathbf{U}^u$ contribution seen in (4) according to the conventional single-path MSDSD algorithm; then, we execute the relay-aided MSDSD based on the matrix $\mathbf{U}$ of (4) according to the conventional single-path MSDSD

algorithm; then, we execute the relay-aided MSDSD based on the matrix $\mathbf{U}$ of (8), which is constituted by combining all the $\{\mathbf{U}^u\}_{u=1}^U$ components.

E. SDB Relay-Aided MSDSD

As stated in Section I, relaxing hard-decision-based detection to its soft-decision-based counterpart will achieve a substantially improved energy-efficiency. To transform the HDB relay-aided MSDSD to its SDB variant, we have to pay particular attention to the *a posteriori* log-likelihood ratio (LLR) of the μth bit $u[\mu]$, given U simultaneously received signal streams represented by $\{\mathbf{z}_u\}_{u=1}^U$, which may be formulated as

$$L\left(u[\mu]\right) = \ln \frac{\Pr\left(u[\mu]=b|\{\mathbf{z}_u\}_{u=1,2,\cdots,U}\right)}{\Pr\left(u[\mu]=\bar{b}|\{\mathbf{z}_u\}_{u=1,2,\cdots,U}\right)}, \ b \in \{0,1\}, \quad (10)$$

where $\bar{b}$ is the complement of b.

We will detail later in Section IV-B that the DN will receive the pair of despread signal streams $\mathbf{z}_s^l$ and $\mathbf{z}_{r_0}^{l+1}$, which correspond to the same SN's transmitted signal stream $\mathbf{S}^l$. Hence, for example, we can substitute $\mathbf{z}_s^l$ and $\mathbf{z}_{r_0}^{l+1}$ into (10) as $\{\mathbf{z}_u\}_{u=1,2}$. As a result, (10) can be rewritten with the aid of Bayes' formula as

$$L\left(u[\mu]\right) = \ln \frac{\Pr\left(u[\mu]=b|\mathbf{z}_s^l,\mathbf{z}_{r_0}^{l+1}\right)}{\Pr\left(u[\mu]=\bar{b}|\mathbf{z}_s^l,\mathbf{z}_{r_0}^{l+1}\right)}$$

$$= \ln \frac{\sum_{\mathbf{V}\in\chi_{:u[\mu]=b}} \Pr\left(\mathbf{z}_s^l|\mathbf{V}\right)\Pr\left(\mathbf{z}_{r_0}^{l+1}|\mathbf{V}\right)\Pr(\mathbf{V})}{\sum_{\mathbf{V}\in\chi_{:u[\mu]=\bar{b}}} \Pr\left(\mathbf{z}_s^l|\mathbf{V}\right)\Pr\left(\mathbf{z}_{r_0}^{l+1}|\mathbf{V}\right)\Pr(\mathbf{V})},$$

$$(11)$$

where the information symbol vector $\mathbf{V}$ consists of $(T_b - 1)$ QPSK symbols. The relationship of the symbol-vector $\mathbf{V}$ and $\mathbf{S}^l$ is also clarified in (1). Furthermore, $\chi_{:u[\mu]=b}$ represents the set of $(M_c^{T_b-1}/2)$ legitimate transmitted vectors $\mathbf{V}$, whose μ^{th} bits are constrained to $u[\mu] = b$, and similarly, $\chi_{:u[\mu]=\bar{b}}$ is defined as the set corresponding to $u[\mu] = \bar{b}$.

The next step is that of substituting the squared Frobenius norm of $\|\mathbf{U}^u\mathbf{S}\|^2$ shown in (4) into (11), where we equivalently represent the probabilities seen in (11) in terms of their associated squared Frobenius norms. Similar manipulations can be found in [66]. In more detail, according to (2), (3) and (4), we arrive at

$$\Pr\left(\mathbf{z}_s^l|\mathbf{V}\right) \propto \exp\left\{-\|\mathbf{U}^s\mathbf{S}^l\|^2\right\},$$

$$\Pr\left(\mathbf{z}_{r_0}^{l+1}|\mathbf{V}\right) \propto \exp\left\{-\|\mathbf{U}^{r_0}\mathbf{S}^l\|^2\right\}. \quad (12)$$

The definition of the matrix $\mathbf{U}^s$ or $\mathbf{U}^{r_0}$ is similar to that stipulated below (4). More particularly, the matrix $\mathbf{U}^s$ is related to $\mathbf{z}_s^l$, while the matrix $\mathbf{U}^{r_0}$ is related to $\mathbf{z}_{r_0}^{l+1}$. Hence, based on (11) and (12) and invoking the "sum-max" approximation

as well as replacing $\mathbf{S}^l$ by the simplified notation of $\mathbf{S}$, the *a posteriori* LLR of $u[\mu]$ is further approximated by

$$L\left(u[\mu]\right)$$
$$\approx \ln \frac{\max_{\mathbf{V}\in\chi_{:u[\mu]=b}}\exp\left\{-\|\mathbf{U}^s\mathbf{S}\|^2-\|\mathbf{U}^{r_0}\mathbf{S}\|^2+\ln\Pr(\mathbf{V})\right\}}{\max_{\mathbf{V}\in\chi_{:u[\mu]=\bar{b}}}\exp\left\{-\|\mathbf{U}^s\mathbf{S}\|^2-\|\mathbf{U}^{r_0}\mathbf{S}\|^2+\ln\Pr(\mathbf{V})\right\}}$$
$$= \underbrace{\left(\left\|\mathbf{U}^s\hat{\mathbf{S}}_{\mathrm{MAP}}^b\right\|^2 + \left\|\mathbf{U}^{r_0}\hat{\mathbf{S}}_{\mathrm{MAP}}^b\right\|^2 - \ln\Pr\left(\hat{\mathbf{V}}_{\mathrm{MAP}}^b\right)\right)}_{\mathrm{MAP\text{-}MSDSD}\in\chi_{:u[\mu]=b}}$$
$$+ \underbrace{\left(\left\|\mathbf{U}^s\hat{\mathbf{S}}_{\mathrm{MAP}}^{\bar{b}}\right\|^2 + \left\|\mathbf{U}^{r_0}\hat{\mathbf{S}}_{\mathrm{MAP}}^{\bar{b}}\right\|^2 - \ln\Pr\left(\hat{\mathbf{V}}_{\mathrm{MAP}}^{\bar{b}}\right)\right)}_{\mathrm{MAP\text{-}MSDSD}\in\chi_{:u[\mu]=\bar{b}}}. \quad (13)$$

The last step is that of performing the calculation of $L(u[\mu])$ of (13) with the aid of the sphere detection process. The evaluation of the *a posteriori* LLR of $L(u[\mu])$ in (13) may be summarized as follows:

1. Let $\hat{\mathbf{S}}_{\mathrm{MAP}}$ denote one of the legitimate differentially encoded DQPSK symbol vectors $\mathbf{S}$, which minimizes the term $\{\|\mathbf{U}^s\mathbf{S}\|^2 + \|\mathbf{U}^{r_0}\mathbf{S}\|^2 - \ln\Pr(\mathbf{V})\}$ involved in the numerator of (13). Then $\hat{\mathbf{V}}_{\mathrm{MAP}}$ represents the corresponding QPSK symbol vector, which is uniquely identified by $\hat{\mathbf{S}}_{\mathrm{MAP}}$. The symbol vector $\hat{\mathbf{S}}_{\mathrm{MAP}}$ may be obtained by implementing a specific sphere detection algorithm, which is an amalgam of the maximum *a posteriori* algorithm called MAP-MSDSD in [62] and of the Relay-Aided MSDSD algorithm described in Section II-D.

2. Employ $\hat{\mathbf{V}}_{\mathrm{MAP}}$ as $\hat{\mathbf{V}}_{\mathrm{MAP}}^b$ and $\hat{\mathbf{S}}_{\mathrm{MAP}}$ as $\hat{\mathbf{S}}_{\mathrm{MAP}}^b$. Correspondingly, the detected value of the μth bit of $\hat{\mathbf{V}}_{\mathrm{MAP}}$ is assigned to the variable b in (13). As a result, both the value of $\bar{b}$ and the reduced-size search space of $\chi_{:u[\mu]=\bar{b}}$ are determined.

3. Implement a constrained MAP-MSDSD algorithm for the sake of seeking $\hat{\mathbf{V}}_{\mathrm{MAP}}^{\bar{b}}$ and $\hat{\mathbf{S}}_{\mathrm{MAP}}^{\bar{b}}$, which is similar to the search process implemented during Step.1. However, this time, the search space is reduced to $\chi_{:u[\mu]=\bar{b}}$. Correspondingly, the associated $\hat{\mathbf{V}}_{\mathrm{MAP}}^{\bar{b}}$ and $\hat{\mathbf{S}}_{\mathrm{MAP}}^{\bar{b}}$ is obtained.

4. On substituting the resulting vectors $\hat{\mathbf{V}}_{\mathrm{MAP}}^b$, $\hat{\mathbf{S}}_{\mathrm{MAP}}^b$, $\hat{\mathbf{V}}_{\mathrm{MAP}}^{\bar{b}}$ and $\hat{\mathbf{S}}_{\mathrm{MAP}}^{\bar{b}}$ into (13), the *a posteriori* LLR of $u[\mu]$ is obtained.

III. SUCCESSIVE AF RELAYING AIDED DS-CDMA UPLINK

A. Successive AF Relaying Aided Single-User DS-CDMA Uplink: Spread-Despread Strategy and Employing Relay-Aided MSDSD

In this section, we focus our attention on the successive AF relaying aided single-user DS-CDMA uplink, where the specific DS-CDMA spreading-despreading strategy designed for appropriately suppressing the CCI is highlighted.

We consider the successive relaying induced CCI problem reported in [46] and [34], which is imposed by the signals directly transmitted by the SN and the signals forwarded by one of the two RNs, both of which are assumed to be simultaneously received at the DN, as depicted in "Phase 1" and "Phase 2" of Fig. 5. Hence, the algorithm discussed in [77] constitutes
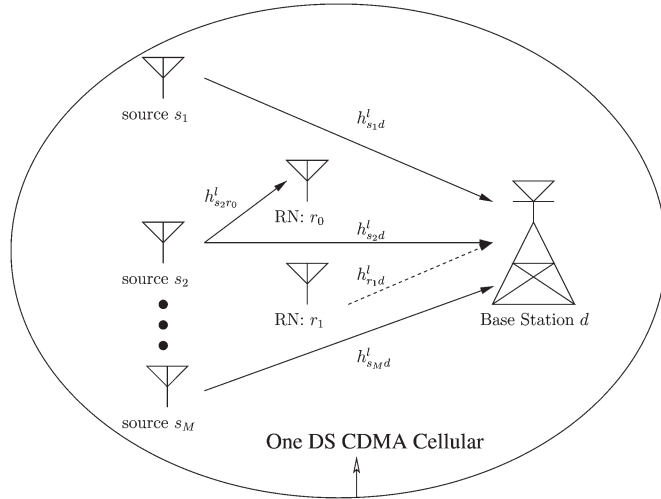
Fig. 17. A simplified uplink diagram of successive AF relaying aided DS-CDMA, assuming that the successive relaying aided cooperative sub-system is embedded in the middle.

a beneficial technique for extracting the different components of the resulting composite signal. Inspired by this concept, the DS-CDMA technique was considered in [77] for suppressing the successive relaying induced CCI, which however has to be further developed for employment in the SRAN of [46], seen in Fig. 18.

Consequently, based on [69], a specific successive AF relaying aided DS-CDMA uplink is portrayed in Fig. 17, where s_n, $n \in \{1, 2, \ldots, M\}$ represent the mobile stations (MSs) and h_{ab}^l, $a, b \in \{s_n, r_0, r_1, d\}$ represent the CIRs spanning from node a to node b during the lth frame. In [69], it was assumed that some of the idle MSs are willing to act as the relays r_0, r_1 and they exclusively assist one of the M users seen on the left hand side of Fig. 17 based on the successive relaying protocol of [46]. It was also assumed in [69] that the impact of the successive relaying induced IRI reported in [46] is negligible, in other words, relay r_0 shown in Fig. 17 is assumed to receive no interference from relay r_1 and vice versa. Furthermore, the signals are assumed to be perfectly synchronised, for example using the solution of [78]. The path-loss effects were ignored in [69] for simplicity. Assuming that the overall transmit power of a single-link direct-transmission based system is P_{total}, for the sake of a fair comparison with classic direct communications using no relays, we explicitly stipulate that the transmit power of every node involved in the SRAN obeys the relationship of $P_s + P_{r_i} = P_{\text{total}}, i \in \{0, 1\}$ and $P_s = P_{r_i}, i \in \{0, 1\}$, where P_a denotes the transmit power of node a. To improve the practicability of the solutions reviewed, standard frame-by-frame based transmissions routinely employed in realistic communication networks are considered here. We will use a single phase depicted in Fig. 5 to transmit a single frame, i.e. the length of a transmission frame is identical to the duration of a phase. According to the specific structure of the SRAN described in Section II-A, when employing frame-based transmission, a specific codeword forwarded by the RN will arrive at the DN a frame period later with respect to the directly received replica transmitted by the SN. Hence the system delay is proportional to the frame length L.

Then, a specific DS-CDMA spreading-despreading strategy may be invoked [69], which is described below:

1) All the frames are divided into even frames ($l = 0, 2, 4, \cdots$) and odd frames ($l = 1, 3, 5, \cdots$). A pair of pseudo-noise (PN) sequences, namely $\mathbf{C}_0$ and $\mathbf{C}_1$ chosen from the entire spreading sequence family is employed for spreading the signals transmitted by the SN during even frames and odd frames, respectively. For example, as illustrated in Fig. 18, the signal transmitted by the SN s during "Phase 0", namely $S^0[k]$ is spread by the PN sequence $\mathbf{C}_0$. Then, during the consecutive odd phase "Phase 1", the signal $S^1[k]$ is spread by another PN sequence $\mathbf{C}_1$. Then, the PN sequence employed by the SN s during the consecutive even phase "Phase 2" is switched to $\mathbf{C}_0$ again.

2) Thus, this spreading scheme guarantees that the two different components of the kth signal $\mathbf{y}^l[k]$ received at the DN during the lth frame, namely those which correspond to the SN's transmitted signal and to the RN's forwarded signal, respectively, are always spread by different PN sequences. This can be confirmed in "Phase 2" of Fig. 18, where the signal $S^2[k]$ broadcast by the SN s and the signal $S^1[k]$ forwarded by the RN r_1 interfere with each other at the DN d, which leads to CCI. Based on the above-mentioned spreading strategy, the signals $S^2[k]$ and $S^1[k]$ are spread by different PN sequences, namely by $\mathbf{C}_0$ and $\mathbf{C}_1$, respectively.

3) Hence, if the matched filter used for despreading $\mathbf{y}^l[k]$ is matched to the waveform $\mathbf{C}_0$, the signal component of $S^2[k]$ can be extracted from the received signal $\mathbf{y}^l[k]$. Meanwhile, when the matched filter is matched to the waveform $\mathbf{C}_1$, the signal component of $S^1[k]$ can be recovered.

Based on the above-introduced specific DS-CDMA spreading-despreading strategy, at the DN, the different components of the received signal $\mathbf{y}^l[k]$ can be extracted by appropriately configuring the matched filter matched to the different spreading codes. If we arrange for the system to obey the relationships of $i \equiv [(l+1) \bmod 2]; \bar{i} \equiv [l \bmod 2]$ and the matched filter used for despreading $\mathbf{y}^l[k]$ is matched to the waveform $\mathbf{C}_{\bar{i}}$, the signal directly transmitted by the SN will contribute the main component of the despread signal, while the RN's forwarded signal becomes the interference of $I_{r_i d}^l[k]$. The associated output of the chip-waveform matched-filter is represented by $z_s^l[k]$. Let us define $\mathbf{Z}_s^l = [z_s^l[1], z_s^l[2], \ldots, z_s^l[N]]^T$, which corresponds to a length-N M_c-ary DPSK symbol vector broadcast by the SN in Fig. 18 during the lth frame, namely to $\mathbf{S}^l$.

The other symbol vector $\mathbf{S}^l$ will be forwarded by the RN $r_{\bar{i}}$, which arrives at the DN d L symbol periods later in the consecutive $(l+1)^{st}$ frame. Similarly, during the $(l+1)^{st}$ frame, we configure the filter to match the waveform of $\mathbf{C}_{\bar{i}}$. Consequently, the despread signal extracted from $\mathbf{y}^{l+1}[k]$ is dominated by the RN's forwarded signal, while the signal directly transmitted by the SN becomes the CCI of $I_{sd}^{l+1}[k]$. This despread signal is represented by $z_{r_{\bar{i}}}^{l+1}[k]$. Let us also define $\mathbf{Z}_{r_{\bar{i}}}^{l+1} = [z_{r_{\bar{i}}}^{l+1}[1], z_{r_{\bar{i}}}^{l+1}[2], \ldots, z_{r_{\bar{i}}}^{l+1}[N]]^T$.

After completing the despreading of the signals received at the DN d, the next step is to invoke the HDB relay-aided MSDSD
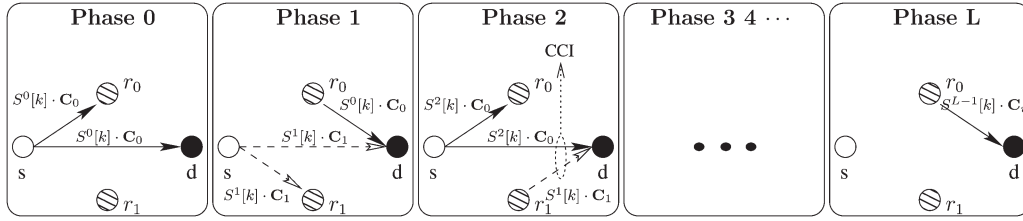
Fig. 18.   The specific DS-CDMA spreading strategy, where $S^l[k]$ represents the kth DPSK symbol of the lth signal frame. The CCI problem is highlighted in "Phase 2". This figure is obtained by applying the above-mentioned DS-CDMA spreading strategy to the relaying regime of Fig. 5.
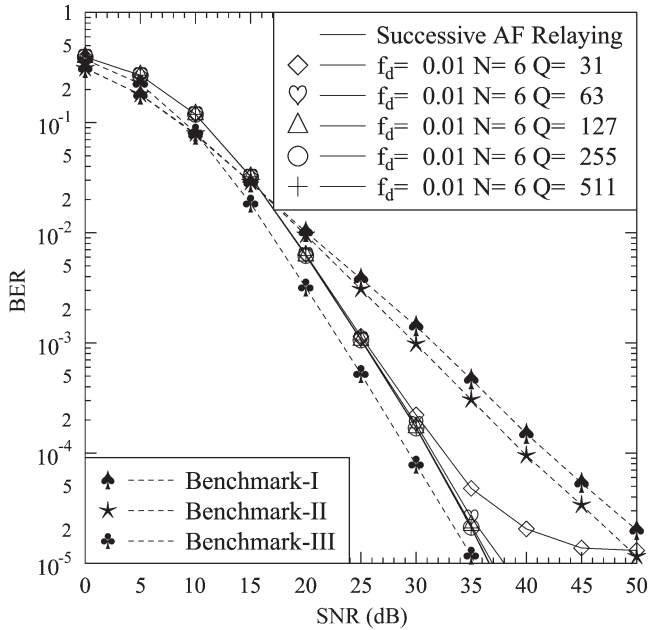

Fig. 19.   BER versus SNR of the successive AF relaying aided single-user DS-CDMA uplink of Fig. 17 employing the HDB relay-aided MSDSD algorithm and using various spreading factors of Q. The interpretations of the three benchmark schemes employed for comparison are given in Table IX.

TABLE VIII
SYSTEM PARAMETERS

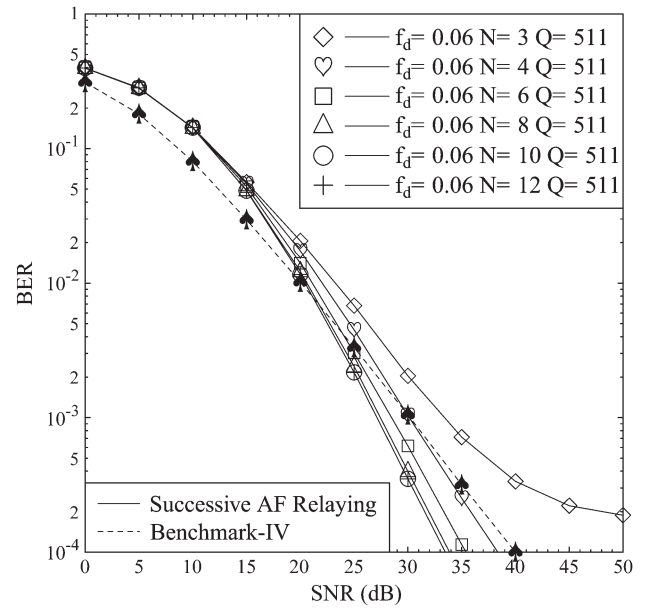| Scenario	Single-User DS-CDMA Uplink
System Regime	Successive AF Relaying
Channel Model	Time-Selective Flat Rayleigh Fading
Normalized Doppler Frequency	$f_d \in \{0.01, 0.06\}$
PN sequence	Gold Sequence
Spreading Factor	$Q \in \{31, 63, 127, 255, 511\}$
Modulation Scheme	Differential QPSK
Demodulation Scheme	HDB Relay-Aided MSDSD
MSDSD Observation Window Size	$N \in \{3, 4, 6, 8, 10, 12\}$

Fig. 20.   Effects of the MSDSD observation window size on the BER performance of the successive AF relaying aided DS-CDMA uplink of Fig. 17 using the parameters of Table VIII.

B. Successive AF Relaying Aided Single-User DS-CDMA Uplink: BER Versus Complexity Performance

Observe in Fig. 13 that conventional two-phase AF relaying operating with the aid of the multiple-path MSDSD algorithm of [68] incurs a severe 50% throughput loss problem. In contrast, the successive AF relaying regime of [46] addressed in Section III-A is capable of recovering the 50% throughput loss. However, this throughput improvement is achieved at the cost of imposing CCI plus the extra amplified and faded noise component on the received signals, which may erode the achievable BER performance gain. This BER performance loss is characterized in Fig. 19. The system parameters used in the simulation results of this section for the sake of substantiating our discussions are based on [69] and are summarized in Table VIII.

algorithm of Fig. 16 introduced in Section II-D for carrying out the noncoherent differential detection at the DN d. Clearly, according to the principle described in Section II-D based on [62] and [79], we can directly implement the HDB relay-aided MSDSD algorithm of [69] by using $\mathbf{Z}_s^l$ and $\mathbf{Z}_{r_i}^{l+1}$ as the $\mathbf{Z}_u$ components in (7). Consequently, the relay-aided MSDSD detection process of the successive AF relaying aided single-user DS-CDMA uplink shown in Fig. 17 becomes feasible.

Specifically, in all the experiments based on the successive AF relaying system characterized in Fig. 19, the normalized Doppler frequency is fixed to $f_d = 0.01$ and the observation window size of the HDB relay-aided MSDSD is fixed to $N = 6$.

Firstly, the impact of the successive relaying induced CCI is quantified, since it significantly affects the system's BER performance. As shown in Fig. 19, increasing the DS-CDMA spreading factor (SF) Q mitigates the influence of the CCI. Nevertheless, an error floor is encountered for a SF of 31 between BER of 10^{-4} and of 10^{-5}. No significant BER improvement can be attained upon increasing the SF beyond 63, but nevertheless a SF of 511 will be adopted in our forthcoming investigations for minimizing the influence of interference in adverse propagation conditions, as justified at a later stage in the context of Fig. 20. Then, the relay-aided MSDSD assisted successive

Benchmark-I	single-user scenario dispensing with relaying	MSDSD [62]	$f_d = 0.01$ $N = 6$
Benchmark-II	single-user scenario dispensing with relaying	coherent DQPSK	$f_d = 0.01$
Benchmark-III	single relay-aided two-phase cooperation	multi-path MSDSD [68]	$f_d = 0.01$ $N = 6$
Benchmark-IV	single-user scenario dispensing with relaying	coherent DQPSK	$f_d = 0.06$

AF system using SF = 511 requires an approximately 2 dB higher transmit power for achieving the target BER of 10^{-4} compared to benchmark-III of Table IX, i.e. in comparison to its counterpart shown in Fig. 13. As stated early in this section, the associated performance degradation seen in Fig. 19 is attributable to two main reasons: firstly, to the successive-relaying-induced CCI between the transmitted signals of the SN and RN; secondly, to the noise component amplified and forwarded by the RN r_i, which is imposed on the despread source signal $z_s^l[k]$ introduced in Section III-A, but would never appear in the Source-to-Destination link of benchmark-III.

According to the comparison of the successive AF relaying system and benchmark-III, we may argue that the successive AF relaying system doubles the spectral efficiency with regard to benchmark-III without substantially degrading the BER performance. On the other hand, the successive AF relaying system substantially outperforms the conventional single-user direct-transmission based schemes operating without RNs, which includes the benchmark-**I** and benchmark-**II**. Hence the successive AF relaying system is capable of striking the most attractive trade-off between the achievable throughput and the attainable BER performance amongst all the schemes listed in Table IX.

As stated in Section II-C, apart from increasing the spatial diversity order for the sake ofreducing the detrimental impact of time-selective fading channels, increasing the observation window size of the MSDSD algorithm is another beneficial method, which results in an improved time diversity. However, when the window size is extended, the complexity imposed increases rapidly. To assess the trade-offs between the attainable time diversity and the system's complexity, simulation results are provided in Figs. 20 and 21, where the normalized Doppler frequency is fixed to $f_d = 0.06$, the spreading factor is fixed to $Q = 511$ and the observation window size N increases from 3 to 12. The remaining parameters are configured according to Table VIII again.

As expected, an increased performance gain is attained when the window size increases from $N = 3$ to 12, as shown in Fig. 20. However, no further significant performance gain may be attained, once the window size reached $N = 8$, despite investing substantially increased search complexity, as quantified in terms of the number of multiplications required for decoding a single symbol. This is particularly so in the low-SNR region, as shown in Fig. 21. In practical applications, the BER should be lower than 10^{-3}. In other words, according to Fig. 20, the new system performs well for SNRs above 30 dB. In this SNR range of Fig. 21, the complexity difference is no longer significant between the different window sizes. This justifies our previous statements, arguing that a window size of $N = 8$ could be a meritorious choice, which has a moderate
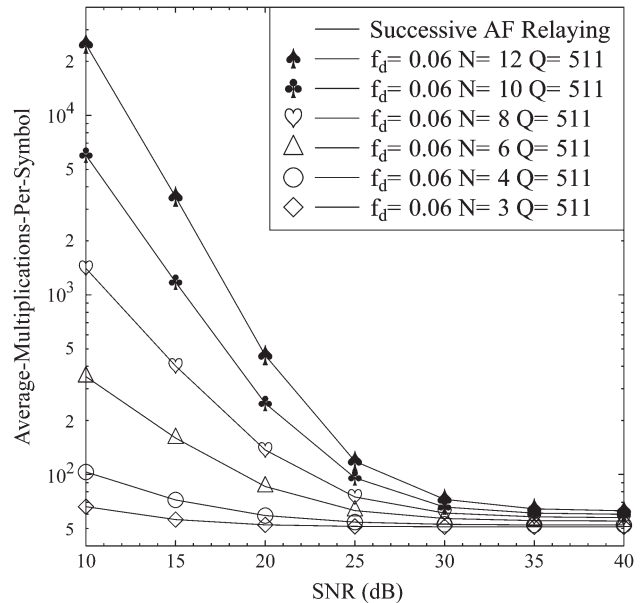

Fig. 21. Complexity versus SNR of the successive AF relaying aided DS-CDMA uplink of Fig. 17 upon varying the observation window size of the HDB relay-aided MSDSD algorithm employed. The system parameters are summarized in Table VIII.

complexity, whilst achieving the best BER performance in the context of the parameters considered.

C. Successive AF Relaying Aided Multi-User DS-CDMA Uplink: Consider CCI, IRI and MAI

In this section, we focus our attention on the successive AF relaying aided multi-user DS-CDMA uplink, where a more realistic scenario is considered, which takes both the IRI as well as the multiple-access interference (MAI) into account. Furthermore, in the spirit of Section III-A, these successive-relaying-induced interferences will be suppressed by relying on the classic DS-CDMA principle upon assigning unique, link-specific spreading codes to the potentially interfering links. Naturally, this implies that the orthogonal time-slots used in [46] are replaced by unique, link-specific CDMA spreading codes at the cost of imposing a soft-limit on the number of users that may be supported, given the limited number of spreading codes.

After extending the single-user DS-CDMA uplink to the more realistic multi-user scenario, the prototype system shown in Fig. 17 is correspondingly replaced by a more generalized network topology, which is portrayed in Fig. 22, where the MS s roaming close to the edge of the DS-CDMA cell activates the SRAN regime to improve its communication quality. In
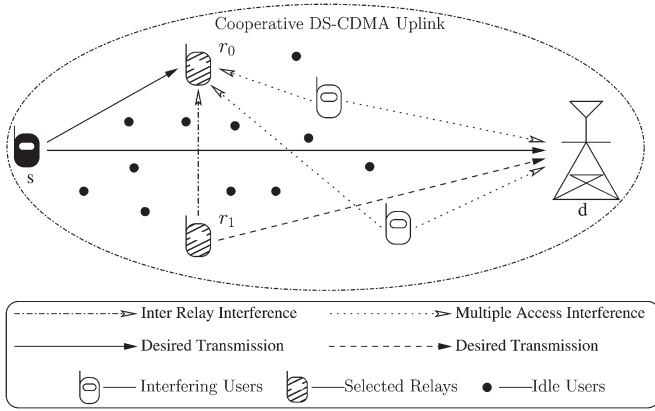
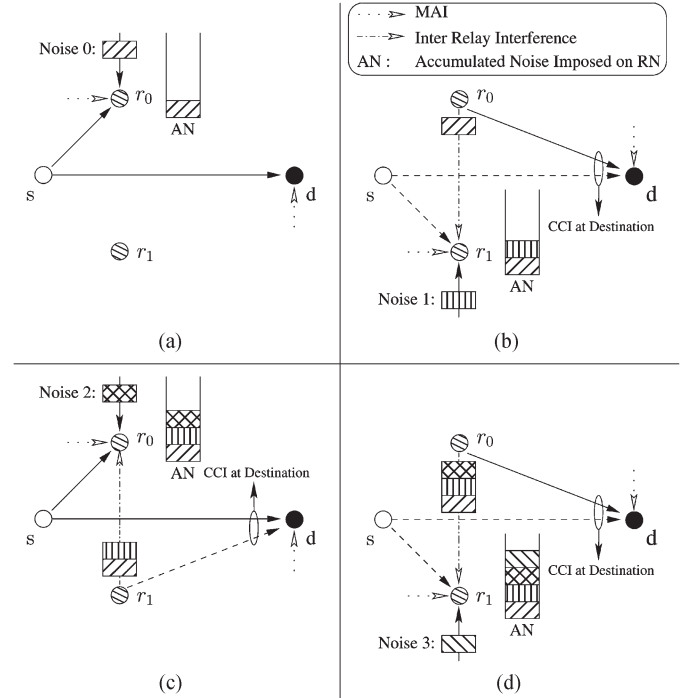Fig. 22. The successive AF relaying aided multi-user DS-CDMA uplink topology.

Fig. 23. The accumulated noise (AN) imposed on the RNs during the successive AF relaying process. (a) Phase 0. (b) Phase 1. (c) Phase 2. (d) Phase 3.

Section III-A, the path-loss effect encountered in realistic systems is ignored for the sake of simplifying the analysis. By contrast, to improve the practicality of the investigations, the path-loss effects are also taken into account from this section onwards. As detailed in [80], the average path-loss reduction gain of the link spanning from node a to node b with respect to the Source-to-Destination link is given by $G_{ab} = (D_{sd}/D_{ab})^{\alpha}, (a, b) \in \{s, r_0, r_1, d\}$, where the notation D_{ab} represents the distance between node a and node b. Throughout this paper, the path-loss exponent is fixed to $\alpha = 3$ for representing a typical urban area. To simplify our analysis, we assume that the SRAN has a symmetric topology, which implies that $D_{sr_0}, D_{r_0d}, G_{sr_0}$ and G_{r_0d} are identical to $D_{sr_1}, D_{r_1d}, G_{sr_1}$ and G_{r_1d}, respectively.

1) Noise Accumulation Problem: In the scenario specified in Section III-A, where the successive relaying induced IRI was not considered, we did not incur the noise accumulation problem either. However, when considering the IRI encountered by our system illustrated in Fig. 22, the noise accumulation problem detailed in this section will occur owing to directly employing the classic AF protocol in the SRAN, where the RN simply amplifies its received signal before retransmitting it. This noise accumulation problem is visualized in Fig. 23. In more detail, the noise accumulation process portrayed in Fig. 23 may be summarised as follows:

1) Observe in "Fig. 23(a) Phase 0" that the RN r_0 receives an AWGN contribution, namely "Noise 0". Hence, at this moment, the AN imposed at the RN r_0 only has a single component: "Noise 0".
2) Observe in "Fig. 23(b) Phase 1" that the RN r_0 simply amplifies all the signal components received during "(a) Phase 0" and then transmits them. Hence, the noise component "Noise 0" is also forwarded to the RN r_1 as part of the IRI. Simultaneously, a new AWGN contribution generated during "Fig. 23(b) Phase 1", namely "Noise 1" is further imposed on the RN r_1. Hence, during "Fig. 23(b) Phase 1", the AN imposed at r_1 increases to two components: "Noise 0" and "Noise 1".
3) Observe in "Fig. 23(c) Phase 2" that the AN consisting of "Noise 0" and "Noise 1", which is imposed on the RN r_1

during the last phase is further forwarded to the RN r_0. Simultaneously, a new AWGN contribution generated during "Fig. 23(c) Phase 2", namely "Noise 2" is also imposed on the RN r_0. Hence, now, the AN imposed on r_0 has three components: "Noise 0", "Noise 1" and "Noise 2".
4) Owing to the same mechanism as stated above, the AN imposed on the RN r_1 will have four components during "Fig. 23(d) Phase 3". Obviously, the accumulated noise imposed on the RNs will continue to increase upon continuing the successive AF relaying transmissions.

Based on the assumption that the power P_s^l of the SN's broadcast signal, the power P_{MAI}^l of the MAI as well as the SNR remain constant for the different frames, and proceeding backwards from the $(l+1)^{st}$ to the 2nd frame of Fig. 23, the variance of the total recursively accumulated noise component in the transmit power $P_{r_i}^{l+1}$ of the RN r_i has been evaluated in [81], which is approximated as

$$\mathbf{Var}[N_{\text{total}}] \approx \sigma^2 f_{AM_{r_i}}^2 \lim_{l \to \infty} \sum_{n=0}^{l-1} \left(f_{AM_{r_i}}^2 G_{r_{\bar{i}}r_i} \right)^n$$

$$= \frac{\sigma^2 f_{AM_{r_i}}^2}{1 - f_{AM_{r_i}}^2 G_{r_{\bar{i}}r_i}}, \qquad (14)$$

where σ^2 is the variance of the AWGN. This implies that all the noise generated in different frames at the different relays will be consistently scaled and accumulated during the transmission process of the classic AF based SRAN. Quantitatively, they impose an extra noise component having a variance of

$\sigma^2 f^2_{AM_{r_i}} G_{r_i d} \cdot (1/1 - f^2_{AM_{r_i}} G_{r_{\bar{i}} r_i})$ on the DN,[8] which cannot be mitigated by the single despreading operation at the DN.

2) Interference Suppression Regime: Let γ_{01} denote the cross-correlation (CCL) of the pair of PN sequences $\mathbf{C}_i, i \in \{0, 1\}$ illustrated in Fig. 18. Observe at "Phase 0" of Fig. 18 that the signal component $S^0[k] \cdot \mathbf{C}_0$ is received at RN r_0. After despreading it at the DN d by $\mathbf{C}_1^T$ at the ensuing "Phase 1", this signal component becomes $S^0[k] \cdot \mathbf{C}_0 \cdot \mathbf{C}_1^T = S^0[k]\gamma_{01}$, which implies that the interfering signal $S^0[k]$ is effectively mitigated by a factor of γ_{01}.

Superimposed on the signal component $S^0[k] \cdot \mathbf{C}_0$, an AWGN vector $\mathbf{n}[k]$ consisting of Q chip-related AWGN samples $n[(k-1)Q+q]$ is also received at RN r_0 during "Phase 0", which may be formulated as [75]: $\mathbf{n}[k] = [n[(k-1)Q+1], n[(k-1)Q+2], \cdots, n[(k-1)Q+Q]]$, where we have $n[(k-1)Q+q] \sim \mathcal{CN}(0, \sigma^2/Q)$. Then, along with despreading the signal component at the DN d by $\mathbf{C}_1^T$ at "Phase 1", the AWGN vector $\mathbf{n}[k]$ is also despread. However, the corresponding term of $\mathbf{n}[k]$ is given by

$$\eta_1 = \sum_{q_1=1}^{Q} n\left[(k-1)Q+q_1\right] c_1[q_1] \sim \mathcal{CN}(0, \sigma^2), \quad (15)$$

where η_1 is a Gaussian variable, which still has a variance of σ^2. This implies that the power of the AWGN vector $\mathbf{n}[k]$ cannot be reduced by a single combined spread-despread operation. However, if η_1 is further spread by $\mathbf{C}_0$ and then despread by $\mathbf{C}_1^T$, we obtain

$$\eta_2 = \sum_{q_2=1}^{Q} \eta_1 c_0[q_2] c_1[q_2]. \quad (16)$$

Observe that η_1 of (15) is a Gaussian random variable, but each of its realizations becomes a specific value in (16). Hence (16) may be rewritten as

$$\eta_2 = \eta_1 \sum_{q_2=1}^{Q} c_0[q_2] c_1[q_2] = \eta_1 \gamma_{01}. \quad (17)$$

This implies that although the power of the AWGN vector $\mathbf{n}[k]$ cannot be reduced by a single combined spread-despread operation, it can definitely be mitigated by multiple spread-despread operations.

Inspired by the above results, a specifically arranged DS-CDMA spread-despread regime is designed in [82], which is portrayed in Fig. 24 for the sake of circumventing the potential noise accumulation process, and to mitigate both the successive relaying induced interferences and the MAI imposed on the
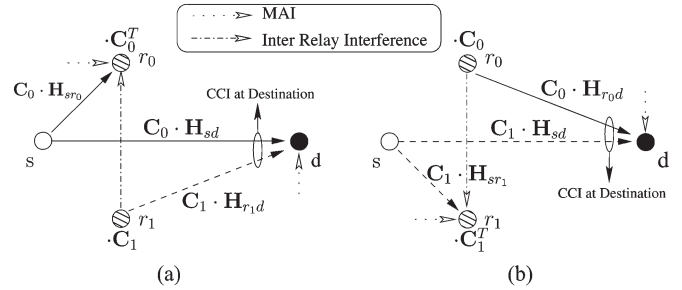

Fig. 24. The generalized successive relaying aided transmission processes and the specific spreading-despreading regime, when considering both the successive relaying induced interferences and the MAI. (a) Even Phase "$l \in \{0, 2, 4 \cdots\}$". (b) Odd Phase "$l \in \{1, 3, 5 \cdots\}$".

cooperative DS-CDMA uplink. This specifically arranged DS-CDMA spreading-despreading regime is detailed as below:

1) At the SN s, the modulated symbols $S^l[k]$ are alternately spread by $\mathbf{C}_0$ and $\mathbf{C}_1$ from frame to frame ($l = 0, 1, \cdots$). For example, observe in Fig. 24 that the signals broadcast by the SN s during the even phases of "$l = 0, 2, 4, \cdots$" are always spread by the PN sequence $\mathbf{C}_0$. By contrast, the signals are still broadcast by the SN s, but during the odd phases of "$l = 1, 3, 5, \cdots$", they are always spread by the other PN sequence $\mathbf{C}_1$.

2) At the RN r_i, the received signals are firstly despread by $\mathbf{C}_i^T$ in its listening mode, and then they are directly spread by $\mathbf{C}_i$ in the transmit mode of the RN r_i before the amplification operation. For example, observe on the left hand side of Fig. 24 that the signal received at the RN r_0 during an even phase, say "Phase 2" is despread by the PN sequence $\mathbf{C}_0^T$. As discussed below (16), after this despreading operation, the noise component imposed on the RN r_0 during "Phase 2" becomes a specific value. Then, the entire signal, which was received and further despread at the RN r_0 during "Phase 2"—including the noise component—is spread by $\mathbf{C}_0$ and then forwarded to the RN r_1 during the consecutive odd phase "Phase 3", as shown in the right hand side of Fig. 24. Hence this noise component inherent in the interfering signal transmitted from the RN r_0 to the RN r_1 will be simultaneously suppressed at the RN r_1 by the despreading operation of $\cdot\mathbf{C}_1^T$ along with the entire interfering signal.

3) Hence, when we employ an appropriate PN sequence for suppressing the interfering signal transmitted by the RNs (e.g. the IRI) at the receiver (RN or DN), according to (17) the AF noise component inherent in the interference will be simultaneously suppressed. This implies that the noise accumulation process is indeed avoided.

4) This spreading-despreading scheme also guarantees that the two different components of the signal received at the DN, namely those which correspond to the SN's transmitted signal and to the RN's forwarded signal, respectively, are always spread by different PN sequences. This is evidenced by observing the pair of signal streams received at the DN d in Fig. 24.

---

[8]It can be proved that $(1 - f^2_{AM_{r_i}} G_{r_{\bar{i}} r_i})$ is always less than 1. Hence we have the relationship that $\sigma^2 f^2_{AM_{r_i}} G_{r_i d} \cdot (1/1 - f^2_{AM_{r_i}} G_{r_{\bar{i}} r_i}) > \sigma^2 f^2_{AM_{r_i}} G_{r_i d}$. Accordingly, the accumulated noise further aggravates the amplified and faded noise problem on the DN incurred in Section III-A.
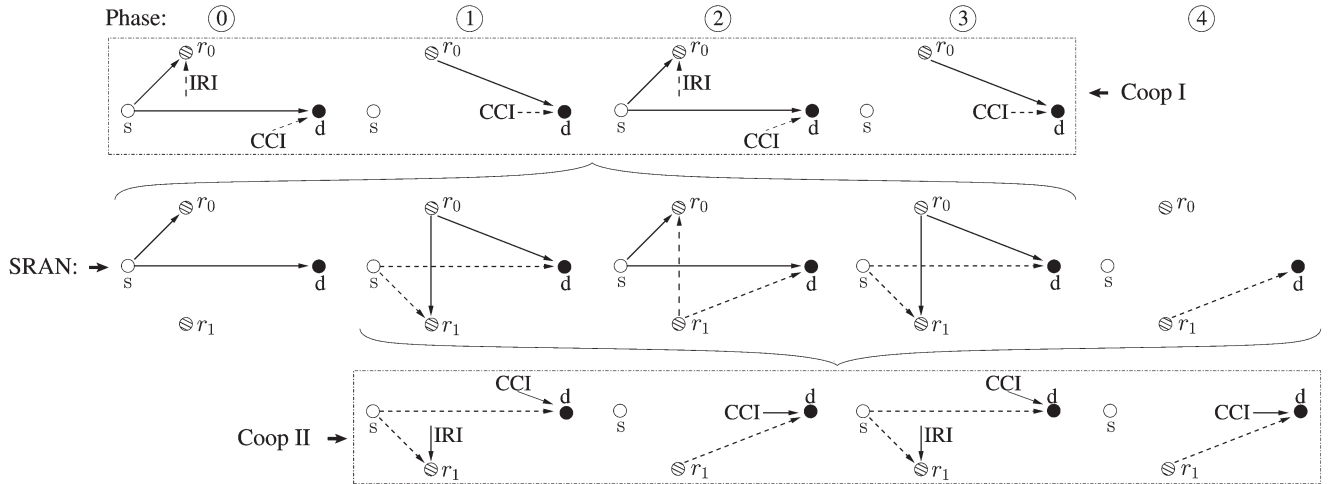
Fig. 25.   Decomposition of the AF based SRAN.

3) Analysis of the Signals Obtained at the DN: Based on the specific interference suppression regime introduced in Section III-C2, we can readily proceed to the analysis of the specific signal components received at the DN. However, for the sake of avoiding complicated mathematical manipulations, in this tutorial paper we refer to [81, Section II.D–E], especially to [81, Eq.(15–16)] for further details of these signal components.

D. Successive AF Relaying Aided Multi-User DS-CDMA Uplink: NC DCMC Capacity

In Section III-B, we focussed our attention on the BER performance versus complexity of the prototype system of Fig. 17 introduced in Section III-A. Based on [82], in this section, we would like to extend our discussions to the theoretical capacity of the prototype system of Fig. 22 introduced in Section III-C. In more detail, based on the idealized simplifying assumption that the CSI is perfectly known, the capacity of the AF based cooperative systems was characterized in [83] and [84]. However, the NC DCMC capacity of the AF based SRAN is still unknown. Hence we focus our attention on the NC DCMC capacity of the successive AF relaying aided multi-user DS-CDMA system herein for characterising its theoretical bound.

The critical issue behind the capacity derivation of the AF based SRAN is that the transmission arrangement of the twin-relay-aided successive relaying procedure of Fig. 24 may be viewed as the superimposed transmissions of two conventional single-relay aided two-phase cooperative links [85]. This has been illustrated in Fig. 24, where the transmissions represented by the solid lines in the even phase and odd phase constitute one of the half-duplex three-terminal cooperative networks, namely Coop-I. Similarly, the transmissions represented by the dashed lines in the even and odd phases constitute another one, namely Coop-II.

To further clarify this decomposition of the AF based SRAN, we illustrate its detailed transmission process in Fig. 25, where the transmissions of the SRAN were split into five phases. Observe in Fig. 25 that the transmission arrangement of the five-phase SRAN may be treated as the superposition of the transmissions of a pair of four-phase based half-duplex three-terminal cooperative networks, which are the above mentioned sub-networks "Coop-I" and "Coop-II". The slight difference between our sub-network "Coop-I" (or "Coop-II") and the conventional half-duplex three-terminal cooperative network is that we additionally imposed the omni-present CCI and IRI on the DN and RN of the sub-networks, respectively, because we have to assume that an equivalent amount of CCI (or IRI) is also imposed on the DN of the sub-networks, just like that which happens to the AF based SRAN located in the middle of Fig. 25.

Hence, we can readily extend the relationship between the AF based SRAN and the pair of half-duplex three-terminal cooperative networks based on Fig. 25 to the generalized scenario, where the transmission arrangement of an $(N + 1)$-phase SRAN may be treated as a superposition of the transmissions of two N-phase half-duplex three-terminal cooperative networks.[9] Hence, assuming that $(N + 1)$ is sufficiently high, we may readily conclude that the noncoherent DCMC capacity of the AF based SRAN is constituted by the sum of the capacities of the AF based sub-network "Coop-I" and "Coop-II", i.e.

$$C_{\text{Successive}}^{\text{AF}} = C_{\text{Coop-I}}^{\text{AF}} + C_{\text{Coop-II}}^{\text{AF}}. \tag{18}$$

Consequently, the problem is transformed to that of deriving the NC DCMC capacity of the AF based half-duplex three-terminal cooperative network e.g. $C_{\text{Coop-I}}^{\text{AF}}$. From a capacity analysis perspective, the sub-network Coop-I may be equivalently modelled by a single-input-multiple-output (SIMO) system having $N_T = 1$ transmit and $N_R = 2$ receive antennas. The evaluation of the NC DCMC capacity of the equivalent SIMO system may be carried out according to the principles introduced in [84]–[86]. Hence, the evaluation of $C_{\text{Successive}}^{\text{AF}}$ in (18) becomes feasible.

---

[9]The transmission arrangements of the first and last phases in the AF based SRAN do not strictly satisfy our decomposition of the AF based SRAN. Nevertheless, when the total number of transmission phases in the AF based SRAN is sufficiently large, we may ignore the slight inaccuracy incurred in the two particular phases.

TABLE X
DISTANCE RATIOS CONSIDERED

θ	D_{sr_i}	$D_{r_i d}$	D_{sd}	$D_{r_0 r_1}$
1/3	1	3	3.824	1
1/2	1	2	2.802	1
1.0	1	1	1.732	1
2.0	2	1	2.802	1
3.0	3	1	3.824	1

TABLE XI
SYSTEM PARAMETERS

Scenario	Multi-User DS-CDMA Uplink
System Regime	Successive AF Relaying
Channel Model	Block Fading Channel [87]
Correlated Fading Block Length	$T_b = 6$
Normalized Doppler Frequency	$f_d = 0.01$
PN sequence	Gold Sequence
Spreading Factor	$Q = 127$
Modulation Scheme	Differential QPSK
Power Allocation	$P_s = P_{r_i} = \frac{1}{2} P_{\text{total}}$
RN's Position	$\theta \in \{\frac{1}{3}, \frac{1}{2}, 1.0, 2.0, 3.0\}$
Number of Interfering Users	$M \in \{0, 32, 64\}$
Ratio of RN's MAI to DN's MAI	$\lambda = 2.0$

In the remaining discussions of this section, we would like to quantify $C_{\text{Successive}}^{\text{AF}}$ with the aid of the associated formulas provided in [81]. Firstly, let us define the distance-ratio of $\theta = (D_{sr_i}/D_{r_i d})$, and assume that $D_{r_0 r_1}$ equals a relatively small value between D_{sr_i} and $D_{r_i d}$. Based on the symmetrical structure of the proposed SRAN assumed in Section III-C, the exact proportions of D_{sr_i}, $D_{r_i d}$, D_{sd} and $D_{r_0 r_1}$ associated with different θ values are summarized in Table X, where the shortest distance is always normalized to unity. Then, let λ represent the ratio of the MAI imposed on the RN r_i to the MAI imposed on the BS. Naturally, the actual value of λ will vary, depending on the specific network topology. As a reasonable value, $\lambda = 2.0$ is assigned in our simulations. Then, the power allocation strategy, the channel model, the correlated block-fading period of T_b, as well as all other system parameters utilized in our forthcoming simulations of this section are summarized in Table XI.

When a cooperative-user-selection scheme is employed, the effect of the RN's position is displayed in Fig. 26, where the RN positions expressed in terms of $\theta \in \{3.0, 2.0, 1.0, (1/2), (1/3)\}$ were considered and the number of interfering users was fixed to $M = 0$. Observe in Fig. 26 that the capacity of the SN's uplink employing the AF based SRAN exceeds that of the conventional SL DT structure, when assigning RNs sufficiently close to the SN. By contrast, it results in a degraded capacity compared to the conventional direct transmission structure, when assigning RNs close to the DN. In our particular case, assigning the RNs at the position $\theta = (1/2)$ is seen to be the best strategy in Fig. 26, which slightly improves the capacity $C_{\text{Successive}}^{\text{AF}}$ compared to the scenarios $\theta = (1/3)$ and $\theta = 1.0$. The capacity of the conventional single-relay aided two-phase AF based cooperative DS-CDMA uplink having $\theta = (1/2)$ is also shown in Fig. 26, which is significantly exceeded by that of its AF based SRAN counterpart.
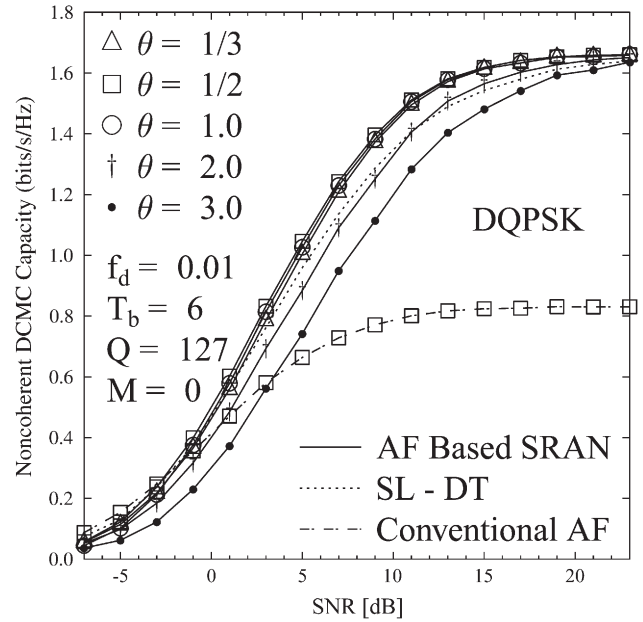
Fig. 26. The effect of the geographic position of the RN on $C_{\text{Successive}}^{\text{AF}}$.
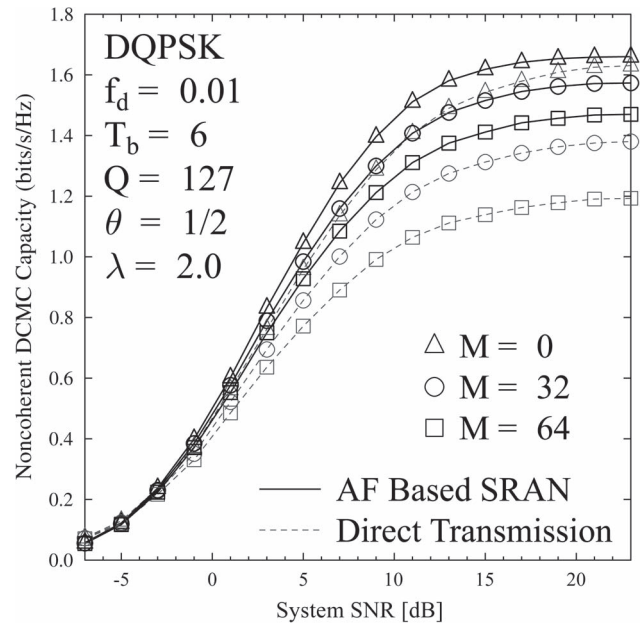
Fig. 27. The noncoherent DCMC capacity $C_{\text{Successive}}^{\text{AF}}$ in zero, moderate and heavy MAI scenarios.

In our next investigation we fix the position of the RNs at $\theta = (1/2)$ and focus our attention on the detrimental effects of having an increased number of interfering users M. Specifically, the values of $M \in \{0, 32, 64\}$ are considered for modelling the scenarios of zero, moderate and heavy MAI, respectively. The relevant simulation results displayed in Fig. 27 demonstrate that the capacity of the AF based SRAN always exceeds that of the direct transmission system, regardless of the number of interfering users. It is more intriguing to find that the capacity advantage of the AF based SRAN with respect to the conventional direct transmission system increases, when the MAI becomes stronger. This implies that in contrast to the

conventional DS-CDMA uplink, the cooperative DS-CDMA uplink will exhibit more substantial advantages in high-load situations.

IV. SUCCESSIVE DF RELAYING AIDED DS-CDMA UPLINK

Based on the interference suppression regime introduced in Section III-A as well as in Section III-C2, it is feasible to efficiently suppress the successive relaying induced interference with the aid of the classic DS-CDMA multiple access technique. Hence, we are capable of operating the SR aided system in a week IRI scenario. Then, according to the analysis provided in Section II-A, especially to the comparisons demonstrated in Fig. 9, we may replace the AF protocol employed in Section III by the DF protocol for the sake of achieving a potentially better BER performance. Therefore, a successive DF relaying aided multi-user DS-CDMA uplink architecture is conceived. Then, the SDB relay-aided MSDSD algorithm introduced in Section II-E can be employed in this system for realizing energy-efficient detection. The resulting DF based SRAN leads to a sophisticated relay-aided SISO-MSDSD assisted three-stage iterative-detection-based transceiver architecture, which will be detailed in Section IV-C.

A. System Model of DF Based SRAN

The network's topology illustrated in Fig. 22 is still valid for the DF based SRAN. Consequently, both the MAI and the successive relaying induced interferences, namely the CCI and IRI contributions are also taken into account in the DF based system model. Furthermore, the relaying-related path-loss reduction effects and the power-allocation as well as the channel model are also assumed to be the same as those defined in Section III-C. All the notation given in Section III will retain the original definitions in this section.

The DS-CDMA based interference suppression regime introduced in Section III-C2 is also valid for the DF based SRAN. In more detail, at the SN s, the modulated symbols $S^l[k]$ are alternately spread by the spreading sequences of $\mathbf{C}_0$ and $\mathbf{C}_1$ from frame to frame ($l = 0, 1, \ldots$). At the RN r_i, the received signals are firstly despread by $\mathbf{C}_i^T$ in the listening mode of RN r_i and then decoded, re-encoded, as well as re-modulated. In the consecutive transmit mode of RN r_i, the re-modulated symbols $\tilde{S}^l[k]$ are always spread by $\mathbf{C}_i$, which are then forwarded to the DN. Again, this spreading scheme is the same to that depicted in Fig. 24, where only the decoding, re-encoding and re-modulating process is omitted. Thus, the spreading scheme also guarantees that the two different components of the signal received at the DN, namely those that correspond to the SN's transmitted signal and to the RN's forwarded signal, respectively, are always spread by different PN sequences.

When employing the DF protocol, the despread signal of the $(l-1)^{st}$ frame at RN r_i associated with $S^{l-1}[k]$ is represented by $y_{r_i}^{l-1}[k]$. At the DN, the received signal is represented by $\mathbf{y}^l[k]$. Hence, similar to the mechanism described in Section III-C3, when the despreading matched-filter is applied to the waveform of $\mathbf{C}_{\bar{i}}$, the signal directly transmitted by

the SN will contribute the main component of the despread signal, while the RN's forwarded signal and the interfering user's signals become the interference. The resulting output of the matched-filter may be represented by $z_s^l[k]$, which corresponds to the information bearing symbol $S^l[k]$. Similar to Section III-A, let us define $\mathbf{Z}_s^l = [z_s^l[1], z_s^l[2], \ldots, z_s^l[N]]^T$, which corresponds to the symbol vector $\mathbf{S}^l = [S^l[1], S^l[2], \ldots, S^l[N]]^T$ broadcast by the SN during the lth frame.

Similarly, when the filter is matched to the waveform $\mathbf{C}_i$, another despread signal can also be extracted from the received signal $\mathbf{y}^l[k]$, which is dominated by the RN's re-modulated symbol[10] $\tilde{S}^l[k]$ and may be represented by $z_{r_i}^l[k]$. If we observe the consecutive $(l+1)$st frame, we obtain $\mathbf{Z}_{r_i}^{l+1} = [z_{r_i}^{l+1}[1], z_{r_i}^{l+1}[1], \ldots, z_{r_i}^{l+1}[N]]^T$, which also corresponds to the symbol vector of $\mathbf{S}^l$. Hence, according to the principles introduced in Section II-E, we can now proceed by implementing the SDB relay-aided MSDSD algorithm at the DN by utilizing $\mathbf{Z}_s^l$ and $\mathbf{Z}_{r_i}^{l+1}$ as the $\mathbf{z}_u$ components in (10).

B. NC DCMC Capacity

As stated at the beginning of this section, the motivation for replacing the AF protocol by the DF protocol is that of achieving a potentially better BER performance. Hence the NC DCMC capacity of the DF based SRAN will be considered in the context of the multi-user DS-CDMA uplink.

The decomposition of the SRAN illustrated in Fig. 25 remains valid for the DF based system model depicted in Section IV-A. Hence, in the spirit of Section III-D, the NC DCMC capacity of the DF based SRAN is also constituted by the sum of the capacities of the pair of sub-networks Coop-I and Coop-II, which is formulated as

$$C_{\text{Successive}}^{\text{DF}} = C_{\text{Coop-I}}^{\text{DF}} + C_{\text{Coop-II}}^{\text{DF}}, \tag{19}$$

where the sub-networks Coop-I and Coop-II illustrated in Fig. 25 of Section III-D now rely on the DF protocol. Then the NC DCMC capacity of these sub-networks can be evaluated according to the principles introduced in [16], [85], [88], and [81]. Hence the evaluation of $C_{\text{Successive}}^{\text{DF}}$ in (19) becomes feasible. Moreover, to compare this DF SRAN capacity to the capacity of the AF based system characterised in Section III-D, the parameters related to the NC DCMC capacity in this section are the same as those specified in Table XI.

The attainable capacity $C_{\text{Successive}}^{\text{DF}}$ associated with different RN positions is shown in Fig. 28. This demonstrates that assigning RNs that roam closer to the SN—rather than to the DN—in the DF based SRAN provides a higher capacity. To expound a little further, in the low SNR region (< 1 dB), the DF based system assigning RNs at the position $\theta = 1.0$ achieves the highest capacity. The phenomenon noted in Section III-D, namely that the capacity gain achieved by replacing the direct

---

[10]The RN receives the information-bearing symbol $S^{l-1}[k]$ during $(l-1)^{st}$ frame. After decoding and re-encoding, the re-modulated symbol $\tilde{S}^l[k]$ is forwarded from the RN to the DN during the lth frame.
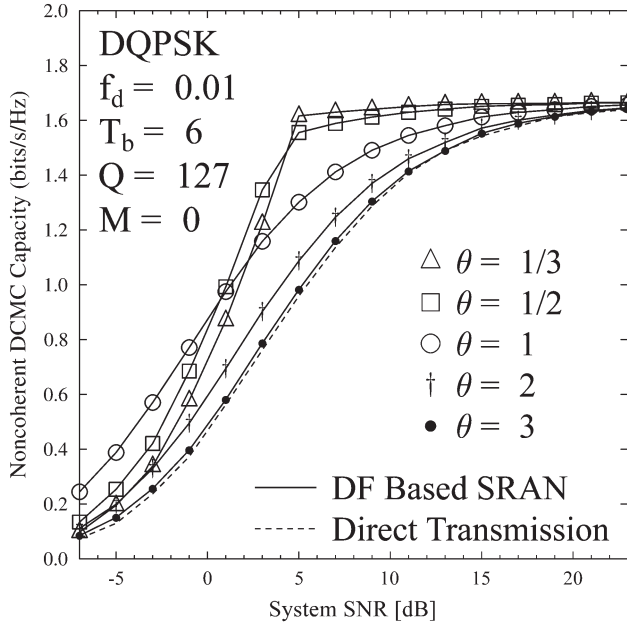
Fig. 28. The effect of the geographic position of the RN on $C_{\text{Successive}}^{\text{DF}}$, as evaluated from (19).
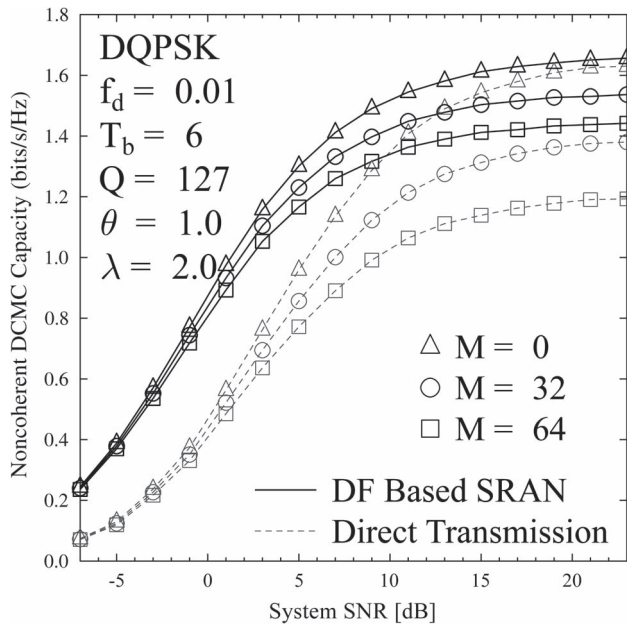

Fig. 29. The noncoherent DCMC capacity $C_{\text{Successive}}^{\text{DF}}$ in zero, moderate and heavy MAI scenarios, as evaluated from (19).

Fig. 30. Schematic of the proposed transceiver in the DF based SRAN.

transmission structure with the SRAN increases upon increasing the number of interfering users remains valid, when considering the DF based SRAN, as demonstrated by Fig. 29. Furthermore, upon comparing Fig. 26 to Fig. 28, we observe that the DF based SRAN assigning appropriate RNs outperforms AF based SRAN, especially at low SNRs, i.e. in the low-throughput region. Hence our objective introduced at the beginning of this section, namely that of improving the system's energy efficiency and/or spectral efficiency by replacing the AF protocol by the DF protocol is indeed achievable.
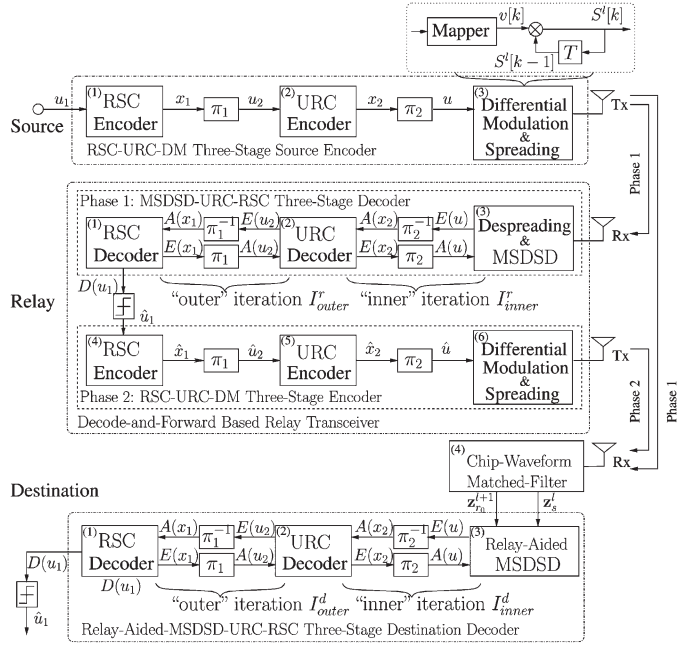
C. Three-Stage Iterative Decoder Design

Based on the relay-aided SISO-MSDSD algorithm addressed in Section II-E, in this section, we design a three-stage iterative detection based transceiver architecture. The complexity of the proposed relay-aided SISO-MSDSD algorithm is characterized at the end of this section.

The transceiver architecture specifically designed for the DF based SRAN is portrayed in Fig. 30. At the SN, we use a conventional differential modulator (DM), such as DQPSK depicted at the top right corner of Fig. 30, which is further combined with a unity-rate-code (URC) encoder to create a two-stage inner code. The URC model has an infinite impulse response due to its recursive encoder structure, consequently the extrinsic information transfer (EXIT) curve [89] of the URC aided inner decoder is capable of approaching the point of perfect convergence at $(1.0, 1.0)$ in the EXIT chart, which is a necessary condition for near-capacity operation [8], [71], and for eliminating the potential error floor phenomenon. Therefore, the receiver of the RN is capable of near-perfectly detecting the information bits $\hat{u}_1$ borne in the signals received from the SN, at as low SNR values as possible. Furthermore, a conventional half-rate recursive systematic convolutional (RSC) code is employed as the outer code. Hence a three-stage RSC-URC-DM source encoder is created.

The corresponding URC decoder assisted three-stage receiver proposed for the relay is also portrayed in Fig. 30. In more detail, the RN's receiver consists of three stages, namely the conventional single-path SISO-MSDSD [66] based soft decoder, the URC decoder and the RSC decoder. The *extrinsic* information and *a priori* information, represented by $E(\cdot)$ and $A(\cdot)$ respectively, are interleaved and iteratively exchanged within the two-stage inner decoder I_{inner}^r times, before the result is further exchanged between the inner and outer decoders I_{outer}^r times. The motivation for employing this
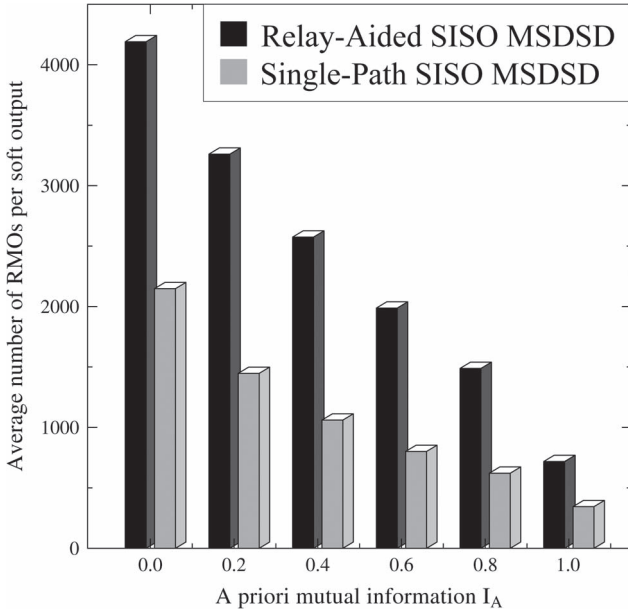
Fig. 31. Complexity comparison between the SDB relay-aided MSDSD decoder and the conventional single-path SISO-MSDSD decoder at different *a priori* mutual information values.

1509 three-stage concatenated decoder architecture is to improve the
1510 convergence behavior of the iterative decoder with the aid of
1511 the URC decoder, as detailed in [8] and [71]. As a benefit,
1512 the error propagation problem of the DF scheme is avoided.
1513 Since the proposed SISO-MSDSD decoder will be employed
1514 at the DN, we have to ensure that its multiple input signal
1515 streams are corresponding to the same differentially modulated
1516 symbols. The RN's transmitter is designed to be identical to the
1517 three-stage RSC-URC-DM encoder of the SN. Hence, observe
1518 at the RN in Fig. 30 that if the estimates $\hat{u}_1$ are correctly
1519 generated by the RN's receiver, the differentially modulated
1520 symbols produced by the RN's transmitter will be the same
1521 as $S^l[k]$.
1522   As seen in Fig. 30, the resulting relay-aided SISO-MSDSD
1523 decoder is employed as the first stage of the iterative receiver
1524 at the DN, which is then further combined with the URC
1525 decoder to form a two-stage inner decoder for appropriately
1526 complementing the SN's and RN's transmitter architecture.
1527 Then, a RSC decoder is concatenated with the relay-aided-
1528 SISO-MSDSD-URC two-stage inner decoder for creating the
1529 DN's three-stage decoder seen in Fig. 30.
1530   Our complexity comparison between the single-path SISO-
1531 MSDSD decoder advocated in [66] and the SDB relay-aided
1532 MSDSD decoder is provided in Fig. 31. In the spirit of [66],
1533 the average number of real-valued multiplication operations
1534 (RMOs) required for generating a single soft-output during the
1535 SDB MSDSD detection once per iteration is employed here
1536 as the complexity measure. For the sake of a fair compari-
1537 son, we ensured that both the conventional single-path SISO-
1538 MSDSD decoder and the SDB relay-aided MSDSD decoder
1539 were operated near their associated "turbo-cliff" points. Then
1540 we varied the *a priori* mutual information of the two different
1541 SDB MSDSD decoders and recorded the associated number
1542 of RMOs required for producing a single soft-output once per

1543 iteration. Observe in Fig. 31 that the SDB relay-aided MSDSD
1544 decoder approximately doubles the complexity compared to
1545 the single-path SISO-MSDSD decoder, which is valid right
1546 across the entire *a priori* mutual information region considered.
1547 The remaining components of the DN's receiver are similar to
1548 those of the RN, hence they affect the overall complexity in a
1549 similar way.
1550   When designing an iterative decoding aided cooperative sys-
1551 tem, the distributed turbo coding scheme advocated in [90] and
1552 [91] is attractive, since it benefits from the iterative information
1553 exchange between the direct and relayed versions of the same
1554 codeword, which experience uncorrelated fading. Naturally,
1555 the improved system performance is achieved at the cost of
1556 increasing the complexity imposed by employing an extra
1557 iteration stage.
1558   By contrast, the relay-aided SISO-MSDSD algorithm consti-
1559 tutes a realistic method of maintaining low complexity, where
1560 the combination of the information provided by the direct and
1561 relayed signal streams, namely by $\mathbf{z}_s^l$ and $\mathbf{z}_{r_0}^{l+1}$ is achieved
1562 without an extra iteration stage. More explicitly, in a cooper-
1563 ative network, where the distributed turbo coding principle is
1564 employed by invoking the single-path SISO-MSDSD [66] al-
1565 gorithm, as in [88], each input signal stream is first individually
1566 processed by a single-path SISO-MSDSD aided turbo decoder
1567 within the inner iterative stage of [88, (Figure 7)]. Then the
1568 resulting information is passed on to the outer iterative stage,
1569 and typically at least two iterations are carried out to exchange
1570 information between the different input signal streams. Hence,
1571 based on our complexity comparisons shown in Fig. 31, it
1572 is reasonable to argue that the three-stage relay-aided-SISO-
1573 MSDSD-URC-RSC decoder is capable of halving the system
1574 complexity imposed by the conventional single-path SISO-
1575 MSDSD aided distributed turbo decoder.

D. Transceiver Performance: Robustness, Throughput and Complexity

1578   In this subsection, we firstly characterise the robustness of
1579 the three-stage relay-aided-SISO-MSDSD-URC-RSC decoder
1580 depicted in Fig. 30 in the terms of its BER performance. We
1581 commence by identifying the "turbo-cliff" SNR with the aid
1582 of EXIT-charts as detailed in [8]. The relevant EXIT-chart and
1583 BER results of the DF based SRAN are shown in Figs. 32 and
1584 33, respectively, when using the system parameters summarized
1585 in Table XII.
1586   Observe in Fig. 32 that an open tunnel exists between the
1587 EXIT curves of the two-stage inner relay-aided-SISO-MSDSD-
1588 URC decoder and the outer RSC decoder, when the overall
1589 equivalent SNR value[11] reaches 2.12 dB. Furthermore, the
1590 associated Monte-Carlo simulation based decoding trajectory
1591 closely matches the EXIT curves. Correspondingly, an in-
1592 finitesimally low BER is expected beyond the SNR = 2.12 dB
1593 point. This is further evidenced in Fig. 33. The capacity of the

---

[11]Here the terminology of "equivalent SNR" is defined as the ratio of
the transmit power to the receiver's noise, which are measured at physically
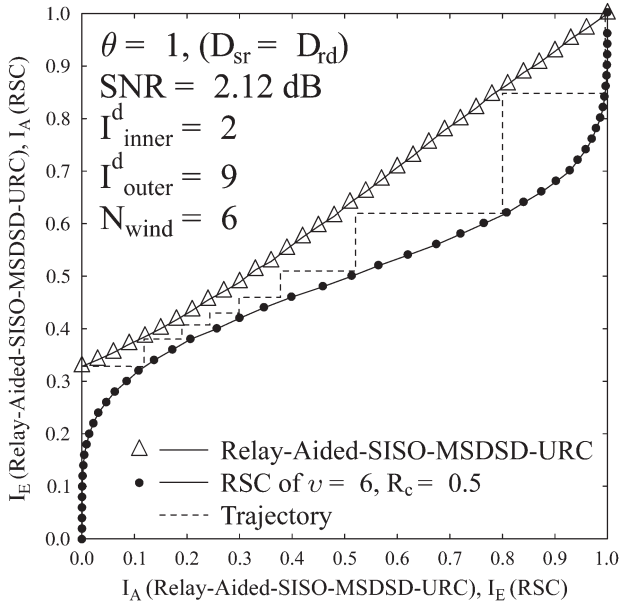different points.

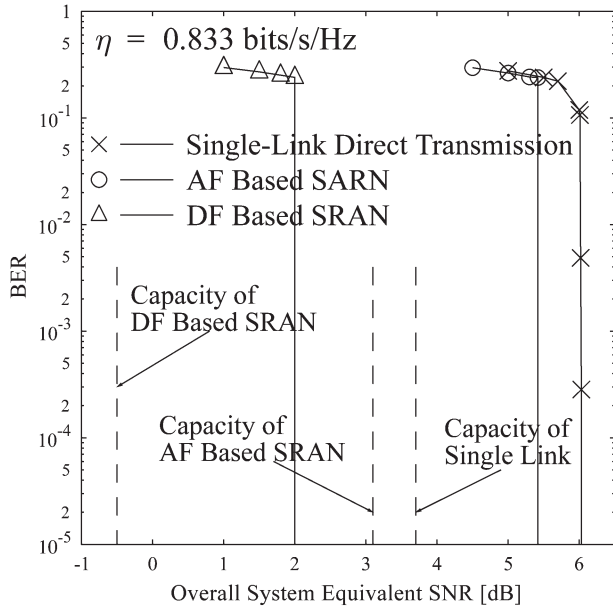Fig. 32. The EXIT characteristic of the three-stage relay-aided-SISO-MSDSD-URC-RSC destination receiver.

TABLE XII
SYSTEM PARAMETERS

Scenario	Multi-User DS-CDMA Uplink
System Regime	Successive DF Relaying
Channel Model	Block Fading Channel [87]
Path-Loss Exponent	$\alpha = 3$
Correlated Fading Block Length	$T_b = 6$
Normalized Doppler Frequency	$f_d = 0.01$
PN Sequence	Gold Sequence
Spreading Factor	$Q = 127$
Channel Coding	RSC Code
Code Memory Length	$\nu = 6$
Code Rate	$R_c = 0.5$
Interleaver Length	4.8×10^5 Symbols
Modulation Scheme	Differential QPSK
MSDSD Window Size	$N_{wind} = 6$
Power Allocation	$P_s = P_{r_i} = \frac{1}{2} P_{\text{total}}$
Inner Iterations of DN's Decoder	$I_{inner}^d = 2$
Outer Iterations of DN's Decoder	$I_{outer}^d = 9$
Relay Position in AF SRAN	$\theta = \frac{1}{2}$, $G_{sr_i} = \left(\frac{1.0}{0.357}\right)^3, G_{r_id} = \left(\frac{1.0}{0.714}\right)^3$
Relay Position in DF SRAN	$\theta = 1.0$, $G_{sr_i} = G_{r_id} = \left(\frac{1.0}{0.577}\right)^3$
Overall Spectral Efficiency	$\eta = 0.8333$ bits/s/Hz

Fig. 33. A comparison of BER performance of different systems.
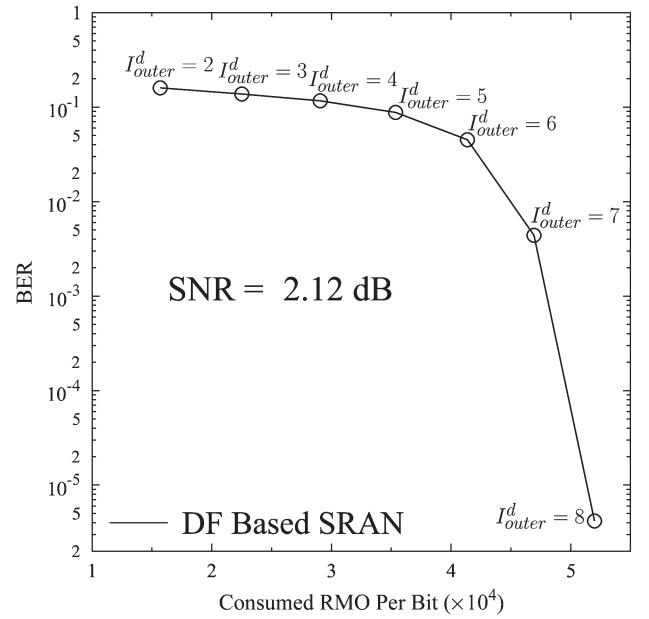
Fig. 34. The BER performance versus the complexity per bit, where the number of outer iterations of the DN's three-stage turbo decoder seen in Fig. 30 increases from $I_{outer}^d = 2$ to $I_{outer}^d = 8$, while the SNR value is fixed at 2.12 dB. The results are based on the schematic of Fig. 30. The remaining parameters employed for generating the results are listed in Table XII.

proposed DF based SRAN is also characterized in Fig. 33, which can be directly obtained from Fig. 28. In our case, the corresponding spectral efficiency is $\eta \approx R_c \times \log_2 M_c \times (T_b - 1/T_b) = 0.8333$ bit/s/Hz. Hence, the proposed transceiver architecture of Fig. 30 attains a performance within 2.6 dB of the capacity of the DF based SRAN.

To elaborate further, observe in Fig. 33 that an approximately 3.9 dB power reduction is achieved by the proposed DF scheme in comparison to the classic direct transmission regime. By contrast, its corresponding AF based counterpart attains a more modest power reduction of about 0.5 dB, which is attained at a lower complexity than that of the DF arrangement.

Then, in Fig. 34, we quantitatively characterize the compromise between the BER performance attained and the extra complexity imposed by the transceiver illustrated in Fig. 30. As expected, Fig. 34 demonstrates that the BER is improved by investing in increased computational complexity in terms of increasing the number of outer iterations. Furthermore, increasing I_{outer}^d to 9 will result in an infinitesimally low BER, as shown in Fig. 32.

Based on the results shown in Fig. 20, it may be anticipated that the energy efficiency of the NC detection aided system architecture of Fig. 30 will be improved by increasing the observation window size of the MSDD algorithms employed.
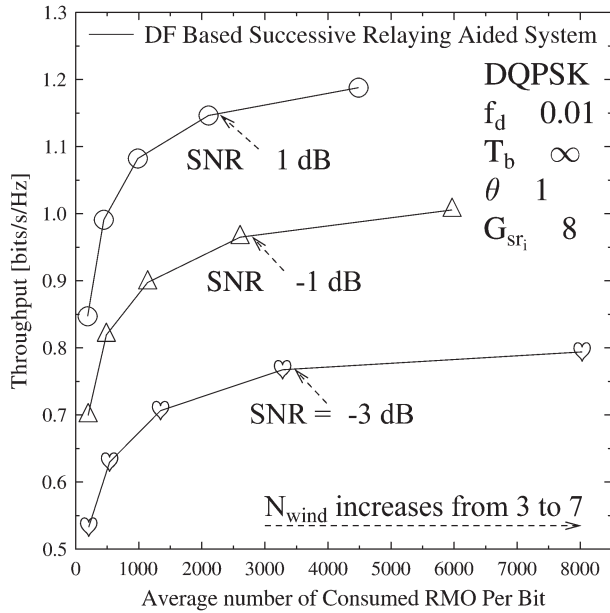
Fig. 35. The trade-off between the maximum achievable throughput and the complexity per bit, where various values of N_{wind} are investigated.

1618 Equivalently, if we fix the transmit power, the system's spectral
1619 efficiency will also benefit from increasing the observation win-
1620 dow size. However, this improvement of the spectral efficiency
1621 is achieved at the cost of imposing an increased complexity on
1622 the system, especially on the MSDD aided decoder, as observed
1623 for example in Fig. 21. Hence we compare the system's com-
1624 plexity imposed by employing different observation window
1625 sizes N_{wind} in the context of the transceiver architecture of
1626 Fig. 30. Then, it can be shown that only the complexity imposed
1627 by increasing the observation window size of the SDB relay-
1628 aided MSDSD decoder has to be involved in the complexity
1629 comparison, where the average number of RMOs required for
1630 producing a single soft-output once per iteration is used again
1631 as the complexity measure.

1632 Consequently, the trade-off between the maximum achiev-
1633 able throughput and the complexity imposed is visualized in
1634 Fig. 35, where different SNR values are considered. In Fig. 35,
1635 the path-loss gain of G_{sr_i} is chosen to be 8, which is different
1636 from that specified in Table XII. As demonstrated in Fig. 35,
1637 when N_{wind} increases from 3 to 5, an efficient trade-off be-
1638 tween the achievable throughput and the complexity imposed
1639 occurs, where the achievable throughput rapidly increases, if
1640 we invest more computational resources. By contrast, with
1641 $N_{\text{wind}} = 5$, the attainable throughput improvement becomes
1642 negligible upon increasing the affordable complexity.

1643   V. CONCLUSIONS AND FUTURE WORK

1644 *A. Summary and Conclusions*

1645   In this paper, we have surveyed noncoherent successive re-
1646 laying techniques for multi-user wireless systems, which are ca-
1647 pable of significantly improving the system's spectral efficiency
1648 by mitigating the half-duplex relaying-induced throughput loss.
1649 Furthermore, they are capable of circumventing the power-

1650 hungry channel estimation process at the cost of the typical 3 dB
1651 power-loss. Hence, in the spirit of our discourse in Section I, the
1652 advocated solutions are capable of striking an attractive com-
1653 promise amongst the conflicting design factors, namely the **ef-
1654 fective throughput**, the **attainable coding gain**, the **bit error
1655 ratio achieved** and the **computational complexity imposed**.

1656   After briefly reciting the relevant history and detailing the
1657 general motivations behind successive relaying and noncoher-
1658 ent detection in Section I, we offered further insights into
1659 the advantages achieved by the SR regimes in Section II-A.
1660 Furthermore, the mathematical derivation of the state-of-the-
1661 art MSDSD algorithms was reviewed in Section II-C, D, E,
1662 respectively. These tutorial reflections introduced Section II,
1663 paving the way for discussing our more sophisticated NC-SR
1664 based prototypes.

1665   In Section III-A and B, the successive AF relaying aided
1666 single-user DS-CDMA uplink was introduced, where the spe-
1667 cific DS-CDMA spreading-despreading strategy was high-
1668 lighted and the signals received at the DN were analysed. As a
1669 benefit of the diversity gain gleaned, this basic prototype system
1670 is capable of reducing the power-dissipation by 8 dB at the
1671 target BER of 10^{-4} compared to the classic "benchmark-II"
1672 of Table IX as shown in Section III-B. Consequently, the BER
1673 performance was improved at the cost of imposing a higher
1674 computational complexity on the system. Then, we further
1675 developed our prototype system from the single-user scenario
1676 to a more realistic multi-user scenario in Section III-C. In
1677 Section III-C1, we revealed the noise accumulation problem
1678 imposed by the IRI in our system, which was mitigated by a
1679 DS-CDMA based interference suppression regime as clarified
1680 in Section III-C2. As a theoretical contribution, the noncoherent
1681 DCMC capacity of the AF multi-user scenario based prototype
1682 system was derived in Section III-D. The DCMC capacity
1683 results of Fig. 26 indicated that the capacity of the AF based
1684 SRAN significantly exceeds that of conventional AF relaying
1685 or that of single-link direct-transmission, provided that RNs
1686 located at the appropriate positions are assigned.

1687   Finally, in Section IV-A, we introduced another prototype
1688 system, namely the successive DF relaying aided multi-user
1689 DS-CDMA uplink, which was developed from the basic pro-
1690 totype introduced in Section III-A for the sake of improving
1691 the system's energy efficiency. The NC DCMC capacity of
1692 the DF based SRAN embedded in the multi-user DS-CDMA
1693 uplink was quantified in Section IV-B. The related simulation
1694 results portrayed in Fig. 28 revealed that the DF based SRAN
1695 outperforms the AF based SRAN, especially in the low-SNR
1696 region (SNR < 0 dB). However, this capacity improvement
1697 with respect to the AF based SRAN introduced in Section III-C
1698 was obtained at the cost of imposing increased complexity at
1699 the RN owing to replacing the AF based RN by the DF based
1700 RN. As a further advance, in Section IV-C, a relay-aided SISO-
1701 MSDSD assisted three-stage iterative transceiver was designed
1702 for efficiently implementing the proposed DF based SRAN. We
1703 observe in Fig. 33 that this transceiver architecture attains a
1704 performance, which is within about 2.6 dB of the DF-based
1705 SRAN's capacity. Again, the fact that the DF based SRAN is
1706 capable of achieving a higher energy efficiency than the AF
1707 based SRAN is illustrated in Fig. 33. However, it is important

TABLE XIII
CRITICAL TECHNIQUES IN SUPPORT OF THE NC-SR AIDED MULTI-USER
WIRELESS SYSTEMS INTRODUCED IN THIS TREATISE

Advanced Techniques	The Sections Involved
Advanced NC detection algorithms	Sections II-C, II-D and II-E
Interference suppression techniques	Sections III-A and III-C
DCMC capacity based characterization	Sections III-D and IV-B
Three-stage turbo decoder designs	Section IV-C
EXIT-chart based analysis	Section IV-D

to remember that this phenomenon relies on the precondition that we operate our SRAN in a weak-IRI scenario.

The salient techniques employed in support of the advocated NC-SR aided multi-user systems are also briefly summarized in Table XIII.

B. Design Guideline

- MIMO techniques have been invoked in support of the operational 3G or 4G wireless communication standards. However, a crucial condition to be satisfied for achieving the spatial diversity gain promised by the family of MIMO techniques is that the multiple co-located antenna elements have to be sufficiently far apart for the sake of experiencing independent fading. To circumvent this limitation, we can rely on the cooperative communication techniques, where the single-antenna-based mobiles, which are sufficiently far apart may form a VAA.

- However, the conventional three-terminal, two-phase based cooperative systems impose a severe 50% multiplexing loss due to the half-duplex transmit/receive modes of practical contemporary transceivers.

- To recover the 50% throughput loss of half-duplex relaying, we may advocate the successive relaying regime of Section II-A. The main idea is to use a pair of half-duplex relays for mimicking a full-duplex relay.

- On the other hand, in support of a coherent cooperative system having a large number of propagation paths owing to employing multiple RNs, the estimation of the large number of channels involved will significantly increase the computational complexity, whilst imposing a high pilot overhead, especially at high normalized Doppler frequencies. Furthermore, it is somewhat unrealistic to expect that in addition to the task of relaying, the relay could altruistically afford to carry out the complex and power-hungry channel estimation of the source-to-relay link in support of coherent detection.

- Against this background, in the context of cooperative communication, we may propose the employment of noncoherent detection for the sake of operating without any requirement of channel estimation.

- Compared to the CDD or MSDD algorithms, the cluster of MSDSD algorithms strikes an attractive trade-off between the BER performance attained and the complexity imposed, which may be considered as a state-of-the-art family of noncoherent detection techniques.

- Given the above-mentioned advantages of successive relaying and the associated MSDSD algorithms, we may beneficially combine them for the sake of constituting an attractive solution, which is capable of circumventing both the 50% throughput loss and the power-hungry channel estimation. Then, to suppress the successive relaying induced interferences, we may additionally invoke the classic DS-CDMA technique. Finally, we arrive at the successive AF relaying aided single-user DS-CDMA uplink advocated in Section III-A.

- For the sake of characterizing the impact of diverse sources of interference (MAI, CCI, IRI), we may then extend the communication scenario considered to multi-user scenarios. We may use the noncoherent DCMC capacity bound of the resulting system for quantifying its benefits over its conventional counterparts.

- In contrast to the AF protocol, the DF protocol may achieve a better BER performance, since it is capable of supporting the employment of sophisticated coding schemes. Correspondingly, we designed a sophisticated relay-aided SISO-MSDSD assisted three-stage iterative-detection based transceiver architecture in Section IV-C, which is capable of striking an attractive trade-off between the BER performance attained and the complexity imposed.

C. Future Research

There remain numerous challenging problems associated with the design of NC-SR based wireless communication systems, which need further investigation in the future:

1) The successive relaying induced interference may be mitigated by the classic DS-CDMA technique, despite dispensing with any CSI. However, this is achieved at the expense of a potential user-load reduction for the CDMA system, since each relaying link requires its own unique spreading sequence, rather than relying on a single spreading code. Alternatively, it is possible to suppress the interference in a noncoherent communication system without requiring any extra orthogonal channel resources. This may be realized with the aid of the differential interference suppression (DIS) philosophy of [92]. In particular, a novel amalgam of the adaptive modified Newton algorithm [93] and the SISO-MSDSD algorithm may constitute a powerful state-of-the-art DIS regime. Therefore, we may use the DIS regime for suppressing the successive relaying induced interference.

2) As reported in [94]–[97], the performance of the entire network, especially its DMT can be further improved by allowing more users and relays to join in the co-operation. Inspired by this result, it may be beneficial to further extend the NC-SR based prototype system of Section III-A to the more sophisticated multi-user multi-relay scenarios. Correspondingly, an appropriate solution for efficiently organizing the multiple nodes of a large-scale cooperative wireless network is desired. For the sake of satisfying this demand, we may employ the family of adaptive network coding techniques detailed in [98]–[100]. Consequently, we may create an adaptive network coded successive relaying regime, where an improved DMT can be expected.

TABLE XIV
GLOSSARY

AF	amplify-and-forward
AN	accumulated noise
AWGN	additive white Gaussian noise
BER	bit-error-rate
BS	base station
CCI	co-channel interference
CSI	channel state information
CIR	channel impulse response
CDD	conventional differential detection
CR	conventional relaying
CCL	cross-correlation
DF	decode-and-forward
DN	destination node
DT	direct-transmission
DM	differential modulator
DMT	diversity-multiplexing trade-off
DIS	differential interference suppression
DF-DD	decision-feedback aided differential detection
DS-CDMA	direct-sequence code-decision multiple-access
EXIT	extrinsic information transfer
FD	full-duplex
FNC	Frobenius norm calculation
FDR	full-duplex relaying
Fano-MSDD	MSDD based Fano-algorithm
HD	half-duplex
HDB	hard-decision-based
IRI	inter-relay interference
ISR	IRI to signal power ratio
LLR	log-likelihood ratio
MS	mobile station
MAI	multiple-access interference
MIMO	Multiple-Input Multiple-Output
MSDD	multiple-symbol differential detection
MPSK	M−ary phase-shift keying
MSDSD	multiple-symbol differential sphere detection
M_c-DPSK	M_c-ary differential phase-shift keying
NC	non-coherent
NC-SR	non-coherent successive relaying
PN	pseudo-noise
PDF	probability density function
RN	relay node
RSC	recursive systematic convolutional code
RMO	real-valued multiplication operation
SL	single-link
SN	source node
SI	self-interference
SR	successive relaying
SF	spreading factor
SDB	soft-decision-based
SRAN	successive relaying aided network
SIMO	single-input-multiple-output
SISO	single-input single-output
SISO-MSDSD	soft-input soft-output MSDSD
URC	unity-rate-code
VAA	virtual antenna array

3) It has been demonstrated in numerous studies [16], [101] that an appropriate resource allocation is capable of significantly improving the energy efficiency and/or spectral efficiency of cooperative communications. Hence it is desirable to carry out the investigation of the advanced optimal power allocation and optimal rate allocation [102] regimes in the context of our NC successive relaying aided system.

APPENDIX

Glossary see Table XIV.

REFERENCES

[1] D. C. Kilper *et al.*, "Power trends in communication networks," *IEEE J. Sel. Topics Quantum Electron.*, vol. 17, no. 2, pp. 275–284, Mar./Apr. 2011.
[2] S. M. Alamouti, "A simple transmit diversity technique for wireless communications," *IEEE J. Sel. Areas Commun.*, vol. 16, no. 8, pp. 1451–1458, Oct. 1998.
[3] I. E. Telatar, "Capacity of multi-antenna Gaussian channels," *Eur. Trans. Telecommun.*, vol. 10, pp. 585–595, Nov. 1999.
[4] G. Foschini, G. Golden, R. Valenzuela, and P. Wolniansky, "Simplified processing for high spectral efficiency wireless communication employing multi-element arrays," *IEEE J. Sel. Areas Commun.*, vol. 17, no. 11, pp. 1841–1852, Nov. 1999.
[5] L. Zheng and D. N. C. Tse, "Diversity and multiplexing: A fundamental tradeoff in multiple-antenna channels," *IEEE Trans. Inf. Theory*, vol. 49, no. 5, pp. 1073–1096, May 2003.
[6] A. J. Paulraj, D. A. Gore, R. U. Nabar, and H. Bölcskei, "An overview of MIMO communications—A key to gigabit wireless," *Proc. IEEE*, vol. 92, no. 2, pp. 198–218, Feb. 2004.
[7] C. Dubuc, D. Starks, T. Creasy, and Y. Hou, "A MIMO-OFDM prototype for next-generation wireless WANs," *IEEE Commun. Mag.*, vol. 42, no. 12, pp. 82–87, Dec. 2004.
[8] L. Hanzo, O. R. Alamri, M. El-Hajjar, and N. Wu, *Near-Capacity Multi-Functional MIMO Systems: Sphere-Packing, Iterative Detection and Cooperation*. New York, NY, USA: Wiley, 2009, ch. 9.
[9] E. C. Van der Meulen, "Three-terminal communication channels," *Adv. Appl. Probability*, vol. 3, no. 1, pp. 120–154, 1971.
[10] T. M. Cover and A. A. El Gamal, "Capacity theorems for the relay channel," *IEEE Trans. Inf. Theory*, vol. 25, no. 5, pp. 572–584, Sep. 1979.
[11] J. N. Laneman, D. N. C. Tse, and G. W. Wornell, "Cooperative diversity in wireless networks: Efficient protocols and outage behavior," *IEEE Trans. Inf. Theory*, vol. 50, no. 12, pp. 3062–3080, Dec. 2004.
[12] J. N. Laneman and G. W. Wornell, "Distributed space-time-coded protocols for exploiting cooperative diversity in wireless networks," *IEEE Trans. Inf. Theory*, vol. 49, no. 10, pp. 2415–2425, Oct. 2003.
[13] A. Sendonaris, E. Erkip, and B. Aazhang, "User cooperation diversity-part I: System description," *IEEE Trans. Commun.*, vol. 51, no. 11, pp. 1927–1938, Nov. 2003.
[14] A. Sendonaris, E. Erkip, and B. Aazhang, "User cooperation diversity-Part II: Implementation aspects and performance analysis," *IEEE Trans. Commun.*, vol. 51, no. 11, pp. 1939–1948, Nov. 2003.
[15] K. Azarian, H. E. Gamal, and P. Schniter, "On the achievable diversity-multiplexing tradeoff in half-duplex cooperative channels," *IEEE Trans. Inf. Theory*, vol. 51, no. 12, pp. 4152–4172, Dec. 2005.
[16] A. Høst-Madsen and J. Zhang, "Capacity bounds and power allocation for wireless relay channels," *IEEE Trans. Inf. Theory*, vol. 51, no. 6, pp. 2020–2040, Jun. 2005.
[17] A. Bletsas, A. Khisti, D. P. Reed, and A. Lippman, "A simple cooperative diversity method based on network path selection," *IEEE J. Sel. Areas Commun.*, vol. 24, no. 3, pp. 659–672, Mar. 2006.
[18] G. Kramer, M. Gastpar, and P. Gupta, "Cooperative strategies and capacity theorems for relay networks," *IEEE Trans. Inf. Theory*, vol. 51, no. 9, pp. 3037–3063, Sep. 2005.
[19] J. G. Andrews, H. Claussen, M. Dohler, S. Rangan, and M. C. Reed, "Femtocells: Past, present, and future," *IEEE J. Sel. Areas Commun.*, vol. 30, no. 3, pp. 497–508, Apr. 2012.
[20] R. U. Nabar, H. Bölcskei, and F. W. Kneubühler, "Fading relay channels: Performance limits and space-time signal design," *IEEE J. Sel. Areas Commun.*, vol. 22, no. 6, pp. 1099–1109, Aug. 2004.
[21] H. Suzuki, K. Itoh, Y. Ebine, and M. Sato, "A booster configuration with adaptive reduction of transmitter-receiver antenna coupling for pager systems," in *Proc. IEEE 50th Veh. Technol. Conf.*, Sep. 1999, pp. 1516–1520.
[22] H. Sakai, T. Oka, and K. Hayashi, "A simple adaptive filter method for cancellation of coupling wave in OFDM signals at SFN relay station," in *Proc. 14th EUSIPCO*, Sep. 2006, pp. 1–5.
[23] K. M. Nasr, J. P. Cosmas, M. Bard, and J. Gledhill, "Performance of an echo canceller and channel estimator for on-channel repeaters in DVB-T/H networks," *IEEE Trans. Broadcast.*, vol. 53, no. 3, pp. 609–618, Sep. 2007.
[24] H. Ju, E. Oh, and D. Hong, "Improving efficiency of resource usage in two-hop full duplex relay systems based on resource sharing and interference cancellation," *IEEE Trans. Wireless Commun.*, vol. 8, no. 8, pp. 3933–3938, Aug. 2009.
[25] J. Sangiamwong, T. Asai, J. Hagiwara, Y. Okumura, and T. Ohya, "Joint multi-filter design for full-duplex MU-MIMO relaying," in *Proc. IEEE 69th Veh. Technol. Conf.*, Apr. 2009, pp. 1–5.

[26] T. Riihonen, S. Werner, and R. Wichman, "Mitigation of loopback self-interference in full-duplex MIMO relays," *IEEE Trans. Signal Process.*, vol. 59, no. 12, pp. 5983–5993, Dec. 2011.

[27] J. I. Choi, M. Jain, K. Srinivasan, P. Levis, and S. Katti, "Achieving single channel, full duplex wireless communication," in *Proc. 16th Annu. Int. Conf. Mobile Comput. Netw.*, 2010, pp. 1–12.

[28] M. Jain *et al.*, "Practical, real-time, full duplex wireless," in *Proc. 17th Annu. Int. Conf. Mobile Comput. Netw.*, 2011, pp. 301–312.

[29] D. Bharadia, E. McMilin, and S. Katti, "Full duplex radios," in *Proc. ACM SIGCOMM*, 2013, pp. 375–386.

[30] T. Riihonen, S. Werner, and R. Wichman, "Comparison of full-duplex and half-duplex modes with a fixed amplify-and-forward relay," in *Proc. IEEE Wireless Commun. Netw. Conf.*, Apr. 2009, pp. 1–5.

[31] T. Riihonen, S. Werner, and R. Wichman, "Hybrid full-duplex/half-duplex relaying with transmit power adaptation," *IEEE Trans. Wireless Commun.*, vol. 10, no. 9, pp. 3074–3085, Sep. 2011.

[32] B. P. Day, A. R. Margetts, D. W. Bliss, and P. Schniter, "Full-duplex MIMO relaying: Achievable rates under limited dynamic range," *IEEE J. Sel. Commun.*, vol. 30, no. 8, pp. 1541–1553, Sep. 2012.

[33] B. Rankov and A. Wittneben, "Spectral efficient signaling for half-duplex relay channels," in *Proc. Conf. Rec. 39th Asilomar Conf. Signals, Syst. Comput.*, 2005, pp. 1066–1071.

[34] B. Rankov and A. Wittneben, "Spectral efficient protocols for half-duplex fading relay channels," *IEEE J. Sel. Areas Commun.*, vol. 25, no. 2, pp. 379–389, Feb. 2007.

[35] P. Popovski and H. Yomo, "Physical network coding in two-way wire-less relay channels," in *Proc. IEEE Int. Conf. Commun.*, Jun. 2007, pp. 707–712.

[36] C. Hausl and J. Hagenauer, "Iterative network and channel decoding for the two-way relay channel," in *Proc. IEEE Int. Conf. Commun.*, Jun. 2006, vol. 4, pp. 1568–1573.

[37] R. Zhang, Y. C. Liang, C. C. Chai, and S. G. Cui, "Optimal beamforming for two-way multi-antenna relay channel with analogue network coding," *IEEE J. Sel. Areas Commun.*, vol. 27, no. 5, pp. 699–712, Jun. 2009.

[38] R. H. Y. Louie, Y. Li, and B. Vucetic, "Practical physical layer network coding for two-way relay channels: Performance analysis and comparison," *IEEE Trans. Wireless Commun.*, vol. 9, no. 2, pp. 764–777, Feb. 2010.

[39] W. Chen, L. Hanzo, and Z. G. Cao, "Network coded modulation for two-way relaying," in *Proc. IEEE Wireless Commun. Netw. Conf.*, Mar. 2011, pp. 1765–1770.

[40] R. Wang and M. Tao, "Joint source and relay precoding designs for MIMO two-way relaying based on MSE criterion," *IEEE Trans. Signal Process.*, vol. 60, no. 3, pp. 1352–1365, Mar. 2012.

[41] P. Popovski and H. Yomo, "Bi-directional amplification of throughput in a wireless multi-hop network," in *Proc. IEEE 63rd Veh. Technol. Conf.*, May 2006, vol. 2, pp. 588–593.

[42] L. Xiao, T. Fuja, J. Kliewer, and D. Costello, "Nested codes with multiple interpretations," in *Proc. 40th Annu. Conf. Inf. Sci. Syst.*, Mar. 2006, pp. 851–856.

[43] T. Oechtering and A. Sezgin, "A new cooperative transmission scheme using the space-time delay code," in *Proc. ITG Workshop Smart Antennas*, Mar. 2004, pp. 41–48.

[44] S. Yang and J. C. Belfiore, "On slotted amplify-and-forward cooperative diversity schemes," in *Proc. IEEE Int. Symp. Inf. Theory*, pp. 2446–2450, Jul. 2006.

[45] S. Yang and J. C. Belfiore, "Towards the optimal amplify-and-forward cooperative diversity scheme," *IEEE Trans. Inf. Theory*, vol. 53, no. 9, pp. 3114–3126, Sep. 2007.

[46] Y. J. Fan, C. Wang, J. S. Thompson, and H. V. Poor, "Recovering multiplexing loss through successive relaying using repetition coding," *IEEE Trans. Commun.*, vol. 6, no. 12, pp. 4484–4493, Dec. 2007.

[47] C. B. Luo, Y. Gong, and F.-C. Zheng, "Interference cancellation in two-path successive relay system with network coding," in *Proc. IEEE 21st Int. Symp. Pers. Indoor Mobile Radio Commun.*, Sep. 2010, pp. 465–469.

[48] C. B. Luo, Y. Gong, and F.-C. Zheng, "Full interference cancellation for two-path relay cooperative networks," *IEEE Trans. Veh. Technol.*, vol. 60, no. 1, pp. 343–347, Jan. 2011.

[49] H. Wicaksana, S. H. Ting, C. K. Ho, W. H. Chin, and Y. L. Guan, "AF two-path half duplex relaying with inter-relay self interference cancellation: Diversity analysis and its improvement," *IEEE Trans. Wireless Commun.*, vol. 8, no. 9, pp. 4720–4729, Sep. 2009.

[50] F. Tian, W. Zhang, W.-K. Ma, P. C. Ching, and H. V. Poor, "An effective distributed space-time code for two-path successive relay networks," *IEEE Trans. Commun.*, vol. 59, no. 8, pp. 2254–2263, Aug. 2011.

[51] E. Başar, U. Aygölü, E. Panayırcı, and H. V. Poor, "A reliable successive relaying protocol," *IEEE Trans. Commun.*, vol. 62, no. 5, pp. 1431–1443, May 2014.

[52] C. I. Bang and M. H. Lee, "An analysis of pilot symbol assisted 16 QAM in the Rayleigh fading channel," *IEEE Trans. Consum. Electron.*, vol. 41, no. 4, pp. 1138–1141, Nov. 1995.

[53] D. Divsalar and M. K. Simon, "Multiple symbol differential detection of MPSK," *IEEE Trans. Commun.*, vol. 38, no. 3, pp. 300–308, Mar. 1990.

[54] K. Mackenthun, "A fast algorithm for multiple-symbol differential detection of MPSK," *IEEE Trans. Commun.*, vol. 42, no. 234, pp. 1471–1474, Apr. 1994.

[55] H. Leib and S. Pasupathy, "The phase of a vector perturbed by Gaussian noise and differentially coherent receivers," *IEEE Trans. Inf. Theory*, vol. 34, no. 6, pp. 1491–1501, Nov. 1988.

[56] F. Edbauer, "Bit error rate of binary and quaternary DPSK signals with multiple differential feedback detection," *IEEE Trans. Commun.*, vol. 40, no. 3, pp. 457–460, Mar. 1992.

[57] F. Adachi and M. Sawahashi, "Decision feedback multiple-symbol differential detection for M-ary DPSK," *Electron. Lett.*, vol. 29, no. 15, pp. 1385–1387, Jul. 1993.

[58] D. Divsalar and M. K. Simon, "Maximum-likelihood differential detection of uncoded and trellis coded amplitude phase modulation over AWGN and fading channels-metrics and performance," *IEEE Trans. Commun.*, vol. 42, no. 1, pp. 76–89, Jan. 1994.

[59] P. Ho and D. Fung, "Error performance of multiple-symbol differential detection of PSK signals transmitted over correlated Rayleigh fading channels," *IEEE Trans. Commun.*, vol. 40, no. 10, pp. 1566–1569, Oct. 1992.

[60] R. Schober, W. H. Gerstacker, and J. B. Huber, "Decision-feedback differential detection of MDPSK for flat rayleigh fading channels," *IEEE Trans. Commun.*, vol. 47, no. 7, pp. 1025–1035, Jul. 1999.

[61] O. Damen, H. E. Gamal, and G. Gaire, "On maximum likelihood detection and the search for the closest lattice point," *IEEE Trans. Inf. Theory*, vol. 49, no. 10, pp. 2389–2402, Oct. 2003.

[62] L. Lampe, R. Schober, V. Pauli, and C. Windpassinger, "Multiple-symbol differential sphere decoding," *IEEE Trans. Commun.*, vol. 53, no. 12, pp. 1981–1985, Dec. 2005.

[63] P. Pun and P. Ho, "The performance of Fano-multiple symbol differential detection," in *Proc. IEEE Int. Conf. Commun.*, May 2005, pp. 2516–2521.

[64] P. Pun and P. Ho, "Fano multiple-symbol differential detectors for differential unitary space-time modulation," *IEEE Trans. Commun.*, vol. 55, no. 3, pp. 540–550, Mar. 2007.

[65] R. M. Fano, "A heuristic discussion of probabilistic decoding," *IEEE Trans. Inf. Theory*, vol. 9, no. 2, pp. 64–74, Apr. 1963.

[66] V. Pauli, L. Lampe, and R. Schober, "Turbo DPSK using soft multiple-symbol differential sphere decoding," *IEEE Trans. Inf. Theory*, vol. 52, no. 4, pp. 1385–1398, Apr. 2006.

[67] L. Wang and L. Hanzo, "The amplify-and-forward cooperative uplink using multiple-symbol differential sphere-detection," *IEEE Signal Process. Lett.*, vol. 16, no. 10, pp. 913–916, Oct. 2009.

[68] L. Wang and L. Hanzo, "Multiple-symbol differential sphere detection for the amplify-and-forward cooperative uplink," in *Proc. IEEE 70th Veh. Technol. Conf.—Fall*, Sep. 2009, pp. 1–5.

[69] L. Li and L. Hanzo, "Multiple-symbol differential sphere detection aided successive relaying in the cooperative DS-CDMA uplink," in *Proc. IEEE Wireless Commun. Netw. Conf.*, Mar. 2011, pp. 1875–1880.

[70] L. Li, L. Wang, and L. Hanzo, "The capacity of successive DF relaying using soft multiple-symbol differential sphere detection," in *Proc. IEEE Global Commun. Conf.*, Dec. 2011, pp. 1–5.

[71] L. Hanzo, Y. Akhtman, M. Jiang, and L. Wang, *MIMO-OFDM for LTE, WIFI and WIMAX: Coherent versus Non-Coherent and Cooperative Turbo-Transceivers*. Hoboken, NJ, USA: Wiley, 2010.

[72] H. Van Trees, *Detection, Estimation and Modulation Theory: Part I*, vol. 6. New York, NY, USA: Wiley, Mar. 1968.

[73] D. Divsalar, M. K. Simon, and M. Shahshahani, "The performance of trellis-coded MDPSK with multiple symbol detection," *IEEE Trans. Commun.*, vol. 38, no. 9, pp. 1391–1403, Sep. 1990.

[74] W. C. Lindsey and M. K. Simon, *Telecommunication Systems Engineering*. Englewood Cliffs, NJ, USA: Prentice-Hall, 1973.

[75] L. Hanzo, L.-L. Yang, E.-L. Kuan, and K. Yen, *Single and Multi-Carrier DS-CDMA: Multi-User Detection, Space-Time Spreading, Synchronisation and Standards*. New York, NY, USA: Wiley, 2005.

[76] E. Agrell, T. Eriksson, A. Vardy, and K. Zeger, "Closest point search in lattices," *IEEE Trans. Inf. Theory*, vol. 48, no. 8, pp. 2201–2214, Aug. 2002.

[77] W. Fang, L.-L. Yang, and L. Hanzo, "Single-user performance of direct-sequence code-division multiple-access using relay diversity and power allocation," *IET Commun.*, vol. 2, no. 3, pp. 462–472, Mar. 2008.

[78] S. Won, K. Lee, and L. Hanzo, "Initial code acquisition in the cooperative noncoherent MIMO DS-CDMA downlink," *IEEE Trans. Veh. Technol.*, vol. 58, no. 3, pp. 1387–1395, Mar. 2009.

[79] A. Abrardo, "Noncoherent MLSE detection of M-DPSK for DS-CDMA wireless systems," *IEEE Trans. Veh. Technol.*, vol. 52, no. 6, pp. 1435–1446, Nov. 2003.

[80] T. S. Rappaport, *Wireless Communications: Principles and Practice*. Upper Saddle River, NJ, USA: Prentice-Hall, 1996.

[81] L. Li, L. Wang, and L. Hanzo, "Successive AF/DF relaying in the cooperative DS-CDMA uplink: Capacity analysis and its system architecture," *IEEE Trans. Veh. Technol.*, vol. 62, no. 2, pp. 655–666, Feb. 2013.

[82] L. Li, L. Wang, and L. Hanzo, "Capacity analysis of the successive AF relaying aided cooperative DS-CDMA uplink," in *Proc. IEEE Wireless Commun. Netw. Conf.*, Apr. 2012, pp. 3057–3062.

[83] Y. Zhao, R. Adve, and T. J. Lim, "Improving amplify-and-forward relay networks: Optimal power allocation versus selection," *IEEE Trans. Wireless Commun.*, vol. 6, no. 8, pp. 3114–3123, Aug. 2007.

[84] Y. W. Ding, J. K. Zhang, and K. M. Wong, "Ergodic channel capacity for the amplify-and-forward half-duplex cooperative systems," *IEEE Trans. Inf. Theory*, vol. 55, no. 2, pp. 713–730, Feb. 2009.

[85] L. K. Kong, S. X. Ng, R. G. Maunder, and L. Hanzo, "Near-capacity cooperative space-time coding employing irregular design and successive relaying," *IEEE Trans. Commun.*, vol. 58, no. 2, pp. 2232–2241, Aug. 2010.

[86] R. Schober and L. Lampe, "Noncoherent receivers for differential space-time modulation," *IEEE Trans. Commun.*, vol. 50, no. 5, pp. 768–777, May 2002.

[87] Y. B. Liang and V. V. Veeravalli, "Capacity of noncoherent time-selective block rayleigh flat-fading channel," in *Proc. IEEE Int. Symp. Inf. Theory*, 2002, p. 166.

[88] L. Wang, L. K. Kong, S. X. Ng, and L. Hanzo, "Code-rate-optimized differentially modulated near-capacity cooperation," *IEEE Trans. Commun.*, vol. 59, no. 8, pp. 2185–2195, Aug. 2011.

[89] A. Ashikhmin, G. Kramer, and S. ten Brink, "Extrinsic information transfer functions: Model and erasure channel properties," *IEEE Trans. Inf. Theory*, vol. 50, no. 11, pp. 2657–2673, Nov. 2004.

[90] B. Zhao and M. C. Valenti, "Distributed turbo coded diversity for relay channel," *Electron. Lett.*, vol. 39, no. 10, pp. 786–787, May 2003.

[91] L. K. Kong, S. X. Ng, R. G. Maunder, and L. Hanzo, "Irregular distributed space-time code design for near-capacity cooperative communications," in *Proc. IEEE Veh. Technol. Conf.*, Sep. 2009, vol. 1, pp. 1–6.

[92] S. K. Cheung and R. Schober, "Differential spatial multiplexing," *IEEE Trans. Wireless Commun.*, vol. 5, no. 8, pp. 2127–2135, Aug. 2006.

[93] J. Yang, F. Yang, H. S. Xi, and W. Guo, "Robust adaptive modified newton algorithm for generalized eigende composition and its application," *EURASIP J. Adv. Signal Process.*, vol. 2007, no. 2, pp. 1–10, Jun. 2007.

[94] J. Kim, D. S. Michalopoulos, and R. Schober, "Diversity analysis of multi-user multi-relay networks," *IEEE Trans. Wireless Commun.*, vol. 10, no. 7, pp. 2380–2389, Jul. 2011.

[95] C. Wang, Y. J. Fan, J. S. Thompson, and H. V. Poor, "A comprehensive study of repetition-coded protocols in multi-user multi-relay networks," *IEEE Trans. Wireless Commun.*, vol. 8, no. 8, pp. 4329–4339, Aug. 2009.

[96] S. Chen, W. Wang, and X. Zhang, "Performance analysis of multiuser diversity in cooperative multi-relay networks under rayleigh-fading channels," *IEEE Trans. Wireless Commun.*, vol. 8, no. 7, pp. 3415–3419, Jul. 2009.

[97] I. Krikidis, J. S. Thompson, S. McLaughlin, and N. Goertz, "Max-min relay selection for legacy amplify-and-forward systems with interference," *IEEE Trans. Wireless Commun.*, vol. 8, no. 6, pp. 3016–3027, Jun. 2009.

[98] X. Bao and J. Li, "Adaptive Network Coded Cooperation (ANCC) for wireless relay networks: Matching code-on-graph with network-on-graph," *IEEE Trans. Wireless Commun.*, vol. 7, no. 2, pp. 574–583, Feb. 2008.

[99] M. Xiao and M. Skoglund, "Multiple-user cooperative communications based on linear network coding," *IEEE Trans. Commun.*, vol. 58, no. 12, pp. 3345–3351, Dec. 2010.

[100] J. L. Rebelatto, B. F. Uchôa-Filho, Y. Li, and B. Vucetic, "Multiuser cooperative diversity through network coding based on classical coding theory," *IEEE Trans. Signal Process.*, vol. 60, no. 2, pp. 916–926, Feb. 2012.

[101] J. W. Huang, Z. Han, M. Chiang, and H. V. Poor, "Auction-based resource allocation for cooperative communications," *IEEE J. Sel. Areas Commun.*, vol. 26, no. 7, pp. 1226–1237, Sep. 2008.

[102] C. Y. Ng, C.-W. Sung, and K. W. Shum, "Rate allocation for cooperative transmission in parallel channels," in *Proc. IEEE Global Commun. Conf.*, 2007, pp. 3921–3925.

Li Li received the Ph.D. degree from Southampton Wireless (SW) Group, School of Electronics and Computer Science, University of Southampton, in October 2013. Upon the completion of the Ph.D. degree, he conducted research as a Senior Research Assistant in the School of Electronics and Computer Science at the University of Southampton from December 2013 to December 2014, where he participated in the European Union Concerto project. In January 2015, he joined the Provincial Key Lab of Information Coding and Transmission, Southwest Jiaotong University, Chengdu, China, serving as a Lecturer.

His research interests include channel coding, iterative detection, noncoherent transmission technologies, cooperative communications and network coding.

H. Vincent Poor (S'72–M'77–SM'82–F'87) received the Ph.D. degree in EECS from Princeton University in 1977. From 1977 until 1990, he was on the faculty of the University of Illinois at Urbana-Champaign. Since 1990, he has been on the faculty at Princeton, where he is the Michael Henry Strater University Professor and Dean of the School of Engineering and Applied Science. He has also held visiting appointments at several universities, including most recently at Stanford and Imperial College. Dr. Poor's research interests are in the area of wireless networks and related fields. Among his publications in these areas is the recent book, *Mechanisms and Games for Dynamic Spectrum Allocation* (Cambridge University Press, 2014).

Dr. Poor is a member of the U. S. National Academy of Engineering and the U. S. National Academy of Sciences, and is a foreign member of Academia Europaea and the Royal Society. He is also a Fellow of the American Academy of Arts and Sciences, the Royal Academy of Engineering (U.K.), and the Royal Society of Edinburgh. He received the Marconi and Armstrong Awards of the IEEE Communications Society in 2007 and 2009, respectively. Recent recognition of his work includes the 2014 URSI Booker Gold Medal, and honorary doctorates from several universities in Asia and Europe.

Lajos Hanzo received the degree in electronics in 1976 and his doctorate in 1983. In 2009, he was awarded the honorary doctorate "Doctor Honoris Causa" by the Technical University of Budapest. During his 35-year career in telecommunications he has held various research and academic posts in Hungary, Germany and the U.K. Since 1986, he has been with the School of Electronics and Computer Science, University of Southampton, U.K., where he holds the chair in telecommunications. He has successfully supervised 80 Ph.D. students, co-authored 20 John Wiley/IEEE Press books on mobile radio communications totalling in excess of 10 000 pages, published 1300 research entries at IEEE Xplore, acted both as TPC and General Chair of IEEE conferences, presented keynote lectures and has been awarded a number of distinctions. Currently, he is directing a 100-strong academic research team, working on a range of research projects in the field of wireless multimedia communications sponsored by industry, the Engineering and Physical Sciences Research Council (EPSRC), U.K., the European IST Programme and the Mobile Virtual Centre of Excellence (VCE), U.K. He is an enthusiastic supporter of industrial and academic liaison and he offers a range of industrial courses. He is also a Governor of the IEEE VTS. During 2008–2012, he was the Editor-in-Chief of the IEEE Press and a Chaired Professor also at Tsinghua University, Beijing. His research is funded by the European Research Council's Senior Research Fellow Grant. For further information on research in progress and associated publications please refer to http://www-mobile.ecs.soton.ac.uk.

AUTHOR QUERIES

AUTHOR PLEASE ANSWER ALL QUERIES

AQ1 = Please provide keywords.
AQ2 = Table VI was cited only in Fig. 12 caption. Please provide citation in text.
AQ3 = Table VII was cited only in Fig. 15 caption. Please provide citation in text.

END OF ALL QUERIES